Lithos 179 (2013) 48–66

Contents lists available at ScienceDirect

Lithos

journal homepage: www.elsevier.com/locate/lithos

Perspectives on the origin of plagiogranite in ophiolites from oxygen isotopes in zircon

Craig B. Grimes [a,*], Takayuki Ushikubo [b], Reinhard Kozdon [b], John W. Valley [b]

[a] Department of Geological Sciences, 1 Ohio University, 316 Clippinger Laboratories, Athens, OH 45701, United States
[b] Department of Geoscience, WiscSIMS, University of Wisconsin, 1215 W. Dayton St., Madison, WI 53706, United States

ARTICLE INFO

Article history:
Received 24 May 2013
Accepted 29 July 2013
Available online 13 August 2013

Keywords:
Oceanic plagiogranite
Dike-gabbro transition
Oxygen isotopes
Ophiolite
Zircon

ABSTRACT

The formation of oceanic plagiogranite has been attributed primarily to either 1) extreme fractional crystallization of a mantle melt, or 2) partial melting of hydrated mafic crust, with support for the latter from field evidence and recent melting experiments. Remelting of hydrothermally-altered ocean crust could yield rocks (and minerals) with diverse primary magmatic $\delta^{18}O$ values forming proximal to the magmatic center where crustal growth is occurring. To constrain the magmatic $\delta^{18}O$ of a wide range of silicic rocks in oceanic crust and evaluate their petrogenesis, we characterized the $\delta^{18}O$ of zircons in 22 plagiogranite samples (tonalite and trondhjemite) from 8 different ophiolites and one dacite sampled along the East Pacific Rise using Secondary Ion Mass Spectrometry (SIMS). The $\delta^{18}O$ values of 202 magmatic zircons from ophiolites range from 3.9 to 5.6‰ ($n = 244$ spots; average 4.9 ± 0.6‰; 2SD), extending ~1‰ below typical zircon in equilibrium with mantle and from gabbroic massifs along slow-spreading mid-ocean ridges (4.7–5.9‰). East Pacific Rise dacite zircons range from 4.6 to 5.0‰ ($n = 12$ spots). Plagiogranite from the dike-gabbro transition zone of the northern Oman Ophiolite yield the lowest $\delta^{18}O$(Zrn), with rock-average values of 4.3–5.0‰. The low-$\delta^{18}O$ values are best explained by remelting of crust altered by hydrothermal fluids with seawater-like isotopic compositions at high temperatures, possibly due to vertical migration of the boundary between an active magma chamber and a vigorous high-temperature hydrothermal system in the overlying crust. If the partial melt was assimilated into a fractionating melt lens with MORB-like $\delta^{18}O$, as envisioned for km-scale plagiogranite bodies in Oman, up to 20% contamination by a protolith with $\delta^{18}O = 2$‰ would be required. Previous oxygen isotope constraints from quartz in Oman plagiogranite suggested melting of both high and low $\delta^{18}O$ crust had occurred; comparison of quartz–zircon pairs indicates that quartz has been modified in most samples, and we find no evidence for the involvement of high-$\delta^{18}O$ rocks during plagiogranite formation.

1. Introduction

Felsic rocks including diorite, trondhjemite, and tonalite are common, albeit minor, constituents of intrusive oceanic crust recovered in drill core and exposed in ophiolites (review by Koepke et al., 2007). Designated collectively as 'oceanic plagiogranite' (Coleman and Donato, 1979; Coleman and Peterman, 1975), these small-volume components are frequent targets for the application of U–Pb zircon geochronology (e.g., Grimes et al., 2008; Jiang et al., 2008; John et al., 2004; Kurth et al., 1998; Tilton et al., 2012; Warren et al., 2005), yielding insights into the magmatic construction of oceanic crust and tectonic history of ophiolites. The processes leading to formation of silicic rocks from mafic oceanic crust have been considered as analogues for the development of felsic crust early in Earth history, particularly during the Hadean (e.g., Bindeman et al., 2012; Rollinson, 2008) although this comparison is complicated by the fact that stable isotope and trace element geochemistry of Hadean zircons is considerably different from zircons in ocean crust (see Bouvier et al., 2012; Grimes et al., 2011a). Other workers have noted a relatively high abundance of oceanic plagiogranite at the dike-gabbro transition of ophiolites, though they occur at all structural levels (e.g., Amri et al., 1996), and interpreted them as evidence for enhanced hydrous partial melting within this narrow horizon where hydrothermal and magmatic systems overlap (France et al., 2010; Gillis and Coogan, 2002; Stakes and Taylor, 1992). While plagiogranite yields insights into a myriad of processes in modern and ancient settings, their petrogenesis has been the subject of much debate.

Most early interpretations of oceanic plagiogranite regarded them as the products of fractional crystallization of basaltic magma at low pressures (e.g., Aldiss, 1981; discussion in Flagler and Spray, 1991), including those exposed within classic ophiolites at Oman (Lippard et al., 1986; Pallister and Hopson, 1981; Pallister and Knight, 1981) and Troodos (Coleman and Peterman, 1975). Reevaluation of many of these same plagiogranite intrusions has led to conclusions that partial melting of hydrothermally altered crust is an important process by which they form, based on studies of field relations, REE geochemical

* Corresponding author. Tel.: +1 740 593 1104.
E-mail address: grimesc1@ohio.edu (C.B. Grimes).

0024-4937/$ – see front matter © 2013 Elsevier B.V. All rights reserved.
http://dx.doi.org/10.1016/j.lithos.2013.07.026

modeling, and comparisons to experimentally-derived high-SiO_2 melts (e.g., Brophy and Pu, 2012; France et al., 2010; Gillis and Coogan, 2002; Koepke et al., 2004, 2007; Rollinson, 2009; Stakes and Taylor, 2003). Flagler and Spray (1991) first proposed an origin for plagiogranite by partial melting of gabbro, related to high-temperature tectonic shearing accompanied be ingress of hydrothermal fluids deep into the crust. More recently, experimental constraints indicate that the preconditioning necessary for anatexis involves reheating of hydrated crust to temperatures in excess of ~850 °C (e.g., France et al., 2010; Koepke et al., 2004).

Plagiogranites are observed in both mid-ocean ridge (MOR) and ophiolite settings, though large-scale intrusions are currently known only from ophiolites (e.g., Aldiss, 1981). Classic examples include decimeter-scale dikes to km-scale plagiogranite bodies in the northern Oman ophiolite associated with composite 'late-intrusive complexes' (e.g., Lippard et al., 1986; Stakes and Taylor, 2003). The large plutons have been interpreted as off-axis intrusions postdating the main stage of crustal construction (Rollinson, 2009; Stakes and Taylor, 2003). The absence of felsic plutons of comparable scale along modern mid-ocean ridges possibly reflects limited drilling within plutonic crust, or differences in the geodynamic setting in which most ophiolites form. Dilek and Furnes (2011) classify two general categories for ophiolites. Subduction-related ophiolites include suprasubduction-zone and volcanic arc types, whereas subduction-unrelated ophiolites include continental margin, mid-ocean ridge, and plume-type ophiolites. Subduction-related ophiolites develop under the influence of fluids derived from dehydration of the subducting slab and melting of metasomatized mantle, and during ascent magmas may interact with older, preexisting crust modified by hydrothermal alteration. These factors could have a significant impact on remelting of the crust.

The oxygen isotope ratio of mantle-derived materials is well established and quite homogeneous (Bindeman, 2008; Eiler, 2001; Mattey et al., 1994; Page et al., 2007b; Valley et al., 1998), and deviations outside the mantle-like range provide clear evidence for subsolidus-alteration or magma contamination by $\delta^{18}O$-modified crust. However, determining primary magmatic $\delta^{18}O$ of altered igneous crust is complicated by the fact that whole rocks and most constituent rock-forming minerals are susceptible to exchange during subsolidus interaction with hydrothermal fluids (Eiler, 2001; Gregory and Taylor, 1981; Muehlenbachs, 1986). The profile through 'typical' ocean crust exhibits elevated $\delta^{18}O$ values of ~+7 to 12‰ in the upper crustal lavas and sheeted diabase dike section, and generally decreases with depth to values between 1 and 6‰ in the lower gabbros (e.g., Alt et al., 1996; Eiler, 2001; Gregory and Taylor, 1981; Stakes et al., 1991). The shift away from the uncontaminated MORB whole rock value (5.6 ± 0.2‰; Eiler, 2001) primarily reflects hydrothermal interactions between seawater-derived hydrothermal fluids and crust at varying temperatures. Exchange with seawater at temperatures of ~300 °C or higher drives $\delta^{18}O$ of the crust to lower values, whereas exchange below ~300 °C shift $\delta^{18}O$ of rocks to higher values (e.g., Alt and Bach, 2006; Gregory and Taylor, 1981). Such large shifts in $\delta^{18}O$ occurring prior to partial remelting and formation of plagiogranite magmas should be evident from the magmatic oxygen isotope ratios of the resultant silicic rocks.

In contrast to most-rock-forming minerals, igneous zircon has been shown to preserve primary magmatic $\delta^{18}O$ very effectively, if not radiation damaged, even when the host rock has experienced extensive alteration or high-grade metamorphism (e.g., Bowman et al., 2011; Page et al., 2007a; Valley, 2003; Valley et al., 2005). In two previous studies of 221 zircons from 46 rocks in the gabbroic section of young oceanic crust (Pb/U zircon ages ranging from 1 to 13 Ma) originating along the slow-spreading Mid-Atlantic and Southwest Indian Ridges, magmatic $\delta^{18}O$ values were found to be extremely uniform and mantle-like with an average of 5.2 ± 0.5‰ (2SD) (Cavosie et al., 2009; Grimes et al., 2011a). These homogeneous $\delta^{18}O$(Zrn) values contrast with the varied whole rock $\delta^{18}O$ values of ~1–10‰ in the same drill cores (Alt and Bach, 2006; McCaig et al., 2010; Stakes et al., 1991), and indicate that the parental magmas did not carry a resolvable seawater signature. Here, we characterize the $\delta^{18}O$ of zircon from 8 different ophiolites, all of which are arguably subduction-related (i.e., Brown et al., 1979; Dilek and Furnes, 2011; Gerlach et al., 1981; Jiang et al., 2008; Köksal et al., 2010; Kurth et al., 1998; Pearce and Robinson, 2010; Zhang et al., 2007). Perhaps the best examples of ophiolite plagiogranite thought to have formed by hydrous partial remelting of mafic crust occupy the dike-gabbro transition of the Oman ophiolite (France et al., 2010; Koepke et al., 2007; Stakes and Taylor, 2003). The dike-gabbro transition preserved in ophiolites has been interpreted as the fossilized interface between a convecting melt lens and vigorous hydrothermal circulation active in the overlying crust (e.g., France et al., 2009; Gillis and Coogan, 2002), thus providing the conditions necessary for partial melting of mafic ocean crust to occur.

2. Samples & geologic background

The objective of this study is to characterize the magmatic oxygen isotope ratio of zircon ($\delta^{18}O$(Zrn)) from plagiogranite in ophiolites, for comparison to lower-crustal mid-ocean ridge (MOR) zircon and further evaluate plagiogranite petrogenesis. Sampling focused on the well-known plagiogranite bodies in the northern part of the Oman ophiolite, including 11 rocks derived from 6 different intrusions (Fig. 1A). The Oman ophiolite samples were originally collected and described by Stakes and Taylor (1992, 2003) and are now part of the collections at the Smithsonian Institute; field descriptions are summarized in Appendix A. Eleven samples from 7 additional ophiolites were surveyed (Fig. 1B) to characterize the variability of $\delta^{18}O$(Zrn) in ophiolite plagiogranite. Field relations and geochemistry of the sample locations have been described previously, and were contributed by authors listed in Table 1. Available whole rock geochemistry is compiled in Table 2. Overall, the whole rocks range in SiO_2 from 58 to 78 wt.%, typically contain 0.1–0.6 wt.% K_2O, and plot as trondhjemite and tonalite on the Ab-An-Or classification (Barker, 1979) (Fig. 2). Brief background descriptions of the ophiolites sampled are provided in Appendix A. A more detailed description of the general geologic setting in which these silicic rocks originated is provided in the following sections, with emphasis on the well-studied Oman ophiolite.

The Oman ophiolite represents one of most well-exposed and continuous subaerial sections of oceanic crust, closely resembling the layered Penrose ophiolite model (Anonymous, 1972). Petrologic and structural evidence suggests that the initial, main phase of ophiolite construction occurred in an extensional setting, however considerable debate has centered around whether it formed dominantly at a mid-ocean ridge or at a suprasubduction zone (SSZ) spreading environment as a result of slab roll-back (e.g., Alabaster et al., 1982; MacLeod et al., 2013; Nicolas and Boudier, 2007; Pearce et al., 1981; Warren et al., 2007). In either case, field relations indicate that the northern portion of the ophiolite formed during multiple magmatic events which were not contemporaneous, and also experienced a complex history of laterally-variable hydrothermal alteration (e.g., Lippard et al., 1986; Stakes and Taylor, 1992). In the northern region, the volcanic sections include lavas with normal MORB chemistry (i.e., V1/Geotimes) overlain by lavas with arc-like petrochemical signatures (i.e., V2) (e.g., Ernewein et al., 1988; Godard et al., 2006). A subduction-influence is inferred from large-ion lithophile element enrichment relative to N-MORB and elevated εSr values reported for quartz-diorite and tonalite from the Lasail plutonic complex, which intrudes the base of V1 volcanics and sheeted diabase dikes (Tsuchiya et al., 2013). Dilek and Furnes (2011) interpret the ophiolite as a suprasubduction-type. A recent compilation of the geochemistry of Oman lavas have been interpreted to indicate high water contents that are incompatible with an origin at a mid-ocean ridge, also leading to the interpretation that Oman formed wholly within a newly formed spreading center above a subduction zone (MacLeod et al., 2013). The southern portion of the Oman ophiolite is less complex and the architecture is often considered as an analogue for crust formed

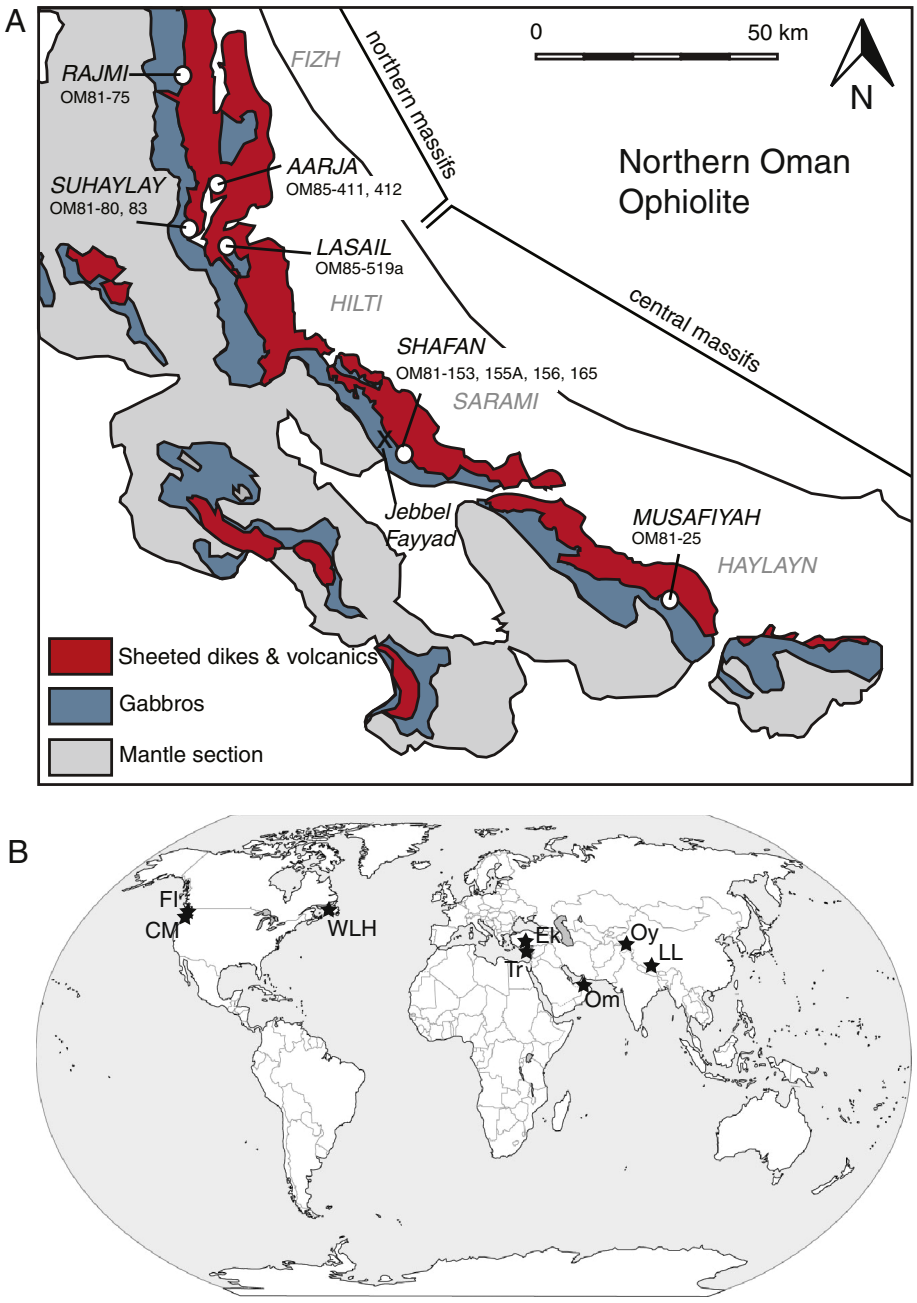

Fig. 1. A) Simplified geologic map of the Oman ophiolite (after Nicolas et al., 2000) showing the location of samples in this study. Samples originate near the sheeted dike-gabbro transition. B) Location of additional ophiolites sampled for comparison to oceanic plagiogranite from the dike-gabbro transition at Oman. CM = Canyon Mountain; FI = Fidalgo Island; WLH = Western Lewis Hills; EK = Ekecikdag; TR = Troodos; OM = Oman; OY = Oytag; LL = Lagkor Lake.

at fast-spreading mid-ocean ridges, however evidence is growing that this analogy may not be entirely appropriate. Subduction-related processes, especially involvement of deep-seated fluids and protracted off-axis magmatic activity, would be significant in the context of hydrous partial remelting and generation of silicic rocks. Other ophiolites incorporated by this study are less controversial, and interpreted as subduction-related ophiolites formed either at a suprasubduction extensional environment or volcanic island arc setting (Table 1).

Plagiogranite occurs throughout the plutonic sections of ocean crust as small, cm-scale dikes and vein networks, but is particularly abundant as late meter-scale to kilometer-scale dikes and plutons into the upper amphibole-bearing gabbros and root zone of the sheeted dike complex of ophiolites (Fig. 3) (e.g., Amri et al., 1996; Coleman and Peterman, 1975; Flagler and Spray, 1991; France et al., 2009; Gillis and Coogan, 2002; Koepke et al., 2007; Lippard et al., 1986; Nicolas et al., 2008; Stakes and Taylor, 2003). At the classic ophiolite localities of Oman and Troodos, the dike-gabbro transition is ~10 to ~100 m thick with underlying amphibole-bearing gabbro giving way to overlying sheeted dikes that have been heavily overprinted by hydrothermal alteration (e.g., France et al., 2009; Gillis and Coogan, 2002; Nicolas et al., 2008; Stakes and Taylor, 1992, 2003). Metamorphic mineral assemblages coupled with stable isotope constraints from ophiolites and fast-spreading oceanic crust indicate that alteration by seawater-derived hydrothermal fluids is pervasive at temperatures up to ~450 °C (e.g., Manning et al., 2000; Stakes and Taylor, 1992). The dike-gabbro transition zone has been interpreted to represent the fossilized roof zone of an axial magma chamber, marking the interface between a fractionating melt lens and a convecting hydrothermal system within the overlying crust (e.g., France et al., 2009; Gillis, 2008; Gillis and Coogan, 2002; Nicolas et al., 2008). Such a horizon would thus be ideal

Table 1
Ophiolite plagiogranite samples analyzed for $\delta^{18}O$(zircon).

Location	Specimen name	SiO_2 (wt.%)	General description[a]	Ophiolite-type	Reference
Oman ophiolite				SSZ (MOR?)	Dilek and Furnes (2011)
Rajmi			Decimeter-scale plagiogranite intruding the base of the sheeted dike complex		Stakes and Taylor, 1992
1	OM81-75	65	Plagiogranite (f, q, ep, amph) cut by epidote veins		Their Fig. 5, loc. 32
Suhaylay			10 km by 8 km intrusion. Lower contact with layered gabbros; upper contact with sheeted-dikes to basalt. Cut in places by late mafic dikes.		Stakes and Taylor, 2003
2	OM81-80	72	Plagiogranite (f, q, sulf, ep, ab, amph, hb, sph)		Their Fig. 4, loc. 343
3	OM81-83	64	Plagiogranite (f, amph, ab, q, mt, ap, hb) from mafic enclave-rich portion		Their Fig. 4, loc. 344
Aarja			1 km-scale intrusion at the gabbro-SDC contact		Stakes and Taylor, 2003
4	OM85–412	71	Plagiogranite (q, ab, ep, op) sampled from near the upper contact with dikes		
5	OM85–411	58	Plagiogranite (f, q, mt, amph) from gabbro margin the lower contact with gabbro; xenoliths, and relict igneous textures present.		Their Fig. 3, loc. 229
Shafan			2–3 km-diameter intrusion at boundary of high-level gabbro & sheeted dikes		Stakes and Taylor, 1992
6	OM81–153		Gabbro (f, hb, ep, cc, sulf, chl, ab, z) from gabbro-plagiogranite contact		Their Fig. 4, loc. 153
7	OM81–155		High level gabbro (f, cpx, hb, amph, q, ep, pr, sulf, ti)		Their Fig. 4, loc. 155
8	OM81–156	64	Plagiogranite (f, q, ep, chl, ap, ab, sph)		Their Fig. 4, loc. 156
9	OM81–165		Pegmatite from gabbro-plagiogranite contact (f, hb, chl, amph, ep, ab, q, pr, ilm, ap)		Their Fig. 4, loc. 162
Lasail			Cm-scale plagiogranite dike within high-level gabbros crosscut by sheeted dikes		Stakes and Taylor, 2003
10	OM85–519a	67	Plagiogranite dike (f, ep, hb, q)		Their Fig. 2, loc. 313
Musafiyah (Wadi Far)			Small segregation dike intruding the high level gabbro-sheeted dike contact		Stakes and Taylor, 2003
11	OM81–25	59	plagiogranite pod (f, q, amph, chl, ep)		
Troodos ophiolite, Cyprus				SSZ	Pearce and Robinson, 2010; Dilek and Furnes, 2011
12	CG10-CY11	74	Meter-scale irregular plagiogranite dikes intruding the lower sheeted dike complex; sampled along the highway 1.5 km N of Zoopigi		
13	CG10-CY3	61	weathered amphibole gabbro pegmatite pods (~30 cm diameter) below the Kakopetria detachment fault (separates underlying gabbros from sheeted dikes above).		
Fidalgo Island ophiolite, WA, USA				Volcanic Arc	Brown et al. (1979)
14	ML-8	70	Decimeter-scale plagiogranite (f, q, amph, ilm, ap)		Unpublished; provided by Nik Christenson
15	ML-3	–	5–10 mm plagiogranite (f, q, chl) dikes cutting amphibole gabbro		Unpublished; provided by Nik Christenson
Western Lewis Hills, Bay of Islands, Newfoundland				Volcanic Arc	Kurth et al. (1998)
16	WLH-22		Undeformed trondjhemite in gabbro from the Western Lewis Hills (island arc)		Kurth et al. (1998)
Ekecikdag area, Turkey				SSZ	Köksal et al. (2010)
17	EK-40	72	(f, q, hb, bt, cpx)		Köksal et al. (2010)
18	EK-41	71	(f, q, hb, bt, cpx)		Köksal et al. (2010)
Canyon Mountain ophiolite, OR, USA				Volcanic Arc	Gerlach et al. (1981)
19	CM-05-1	–			Unpublished; provided by Josh Schwartz
Lagkor Lake ophiolite, Tibet				SSZ	
20	GZ-1	72	Plagiogranite dike cutting gabbro section (f, q, hb, bt, cpx, z, ep)		Zhang et al. (2007)
Oytag ophiolite, western Kunlun orogen, China				Volcanic Arc	
21	WYT-5	78	Pluton intruding the volcanic sequence (f, q, amph, chl, ep, ilm)		Jiang et al. (2008)
22	GZ-1	75	Pluton intruding the volcanic sequence (f, q, amph, chl, ep, ilm)		Jiang et al. (2008)
9°N, East Pacific Rise					
23	265–70	66	Dacite lava sampled within the axial valley	fast spread MOR	Wanless et al. (2011)

[a] Mineral abbreviations (shown in parentheses): f = plagioclase feldspar; q = quartz; hb = hornblende; cpx = clinopyroxene; bt = biotite; amph = green amphibole; chl = chlorite; ep = epidote; ab = albite; pr = prehnite; ilm = ilmenite; ti = titanite; sulf = sulfide; mt = magnetite; ap = apatite.

Table 2
Whole rock geochemistry of ophiolite plagiogranite analyzed for $\delta^{18}O$(Zrn).

	Oman[a]								Troodos		Fidalgo Is.	WLH, Bay of Is.	Ekecikdag	Ekecikdag	Lagkor Lake	Oytag	Oytag	EPR
	OM81-75	OM81-80	OM81-83	OM85-412	OM85-411	OM81-25	OM81-156	OM85-519a	CY11	CY3	ML-8	WLH 22	EK-40	EK-41	GZ-45-1	WYT-5	GZ-1	265-70
	Ragmi	Suhaylah	Suhaylah	Aarja	Aarja	Musafiya	Shafan	Lasail										
wt.%																		
SiO_2	65.4	72.3	63.6	71.1	57.5	59.3	64.5	66.8	73.9	61.4	69.7	71.1	71.8	71.4	71.8	77.9	75.2	66.3
TiO_2	0.98	0.52	1.22	0.46	0.52	1.31	0.69	0.78	0.25	0.56	0.26	0.27	0.30	0.34	0.22	0.14	0.19	0.87
Al_2O_3	15.3	13.7	14.8	12.1	15.2	15.7	16.5	15.3	13.7	18.1	14.1	14.9	14.3	14.1	14.7	11.8	12.1	13.2
Fe_2O_3t	6.69	4.58	7.81	6.70	9.50	9.68	5.16	5.78	4.21	3.90	3.48	4.42	3.28	4.04	2.75	1.87	3.60	7.17
MnO	0.08	0.05	0.12	0.02	0.14	0.12	0.05	0.05	0.00	0.07	0.06	0.07	0.09	0.10	0.04	0.03	0.10	0.14
MgO	1.33	1.35	2.13	0.67	5.28	3.99	1.26	1.41	0.42	3.70	1.48	1.45	0.60	0.82	1.39	0.23	0.38	0.80
CaO	4.15	1.59	3.00	2.10	5.99	4.00	7.69	2.79	2.94	6.39	3.97	2.00	4.11	4.43	2.99	2.04	2.16	3.23
Na_2O	6.24	6.75	7.13	5.10	3.50	5.45	4.47	6.54	4.46	5.48	3.54	5.17	3.81	3.46	3.84	4.81	4.64	4.08
K_2O	0.17	0.37	0.25	0.20	0.42	0.27	0.15	0.38	0.08	0.32	1.58	0.56	0.25	0.49	0.83	0.16	0.53	1.33
P_2O_5	–	–	–	–	3.00	0.16	–	0.18	0.06	0.11	0.03	0.05	0.07	0.07	0.06	0.05	0.06	0.19
LOI	–	–	–	–	–	–	–	–	–	–	1.80	1.50	–	–	1.47	0.71	0.87	–
Total	100.32	101.12	100.10	99.85	101.05	99.84	100.42	99.82	99.94	99.89	100.01	101.49	98.64	99.22	98.63	99.76	99.85	97.27
ppm																		
Sc						22.4		11.3	12.0	18.9			11.0	16.0	4.0	3.8	5.2	12.3
V						262		49	26	116			24	40	31	5	9	45
Cr						1.8		0.2	0.6	25.0					4.9	8.6	15.3	3.7
Ni						9.0		0.6	3.8	23.8		39.0			5.9		4.8	5.0
Rb	1.4	1.4	1.0	9.0	6.0	1.8	0.9	1.3	1.5	1.7			9.1	10.5	8.2	1.1	5.5	15.0
Sr	165	122	148	180	120	207	278	148	136	588			103	81	162	66	62	78
Y	56	69	64	43	24	28	54	50	32	17			25	28	4	77	41	160
Zr	221	211	175	83	52	104	167	206	84	134			54	45	99	200	187	934
Nb						1.2		2.4	1.0	1.1					1.0	2.3	1.7	15.9
Ba						80.3		35.8	26.4	28.5			52.0	58.0	148.8	66.0	55.0	72.7
La						4.4		4.6	6.1	1.4		3.9			4.8	7.8	10.3	30.9
Ce						12.4		14.6	13.8	4.0		9.0			8.9	20.2	22.6	88.2
Pr						2.0		2.5	1.9	0.7					0.9	3.8	3.8	12.5
Nd						10.7		14.0	9.4	3.8		5.9			3.4	20.1	18.1	55.0
Sm						3.37		4.77	3.02	1.38		1.62			0.6	6.6	4.4	16.7
Eu						1.16		1.64	0.88	0.58		0.23			0.5	0.5	1.2	3.1
Gd						4.29		6.56	3.77	1.94		1.56			0.5	9.2	5.5	19.5
Tb						0.79		1.25	0.76	0.37					0.1	1.9	1.1	3.7
Dy						5.54		8.94	5.67	2.73		2.27			0.6	12.5	6.9	25.1
Ho						1.14		1.96	1.24	0.61					0.2	2.9	1.5	5.4
Er						3.20		5.80	3.71	1.83		1.52			0.5	8.9	4.7	16.4
Tm						0.44		0.84	0.53	0.26					0.1	1.4	0.8	2.6
Yb						2.76		5.62	3.40	1.76		1.62			0.6	9.1	5.2	17.5
Lu						0.38		0.80	0.46	0.25		0.24			0.1	1.4	0.9	2.7
Pb						0.57		0.21	1.35	0.43					2.6	1.2	2.0	3.8
Th						0.13		0.32	0.71	0.12					2.1	1.7	2.1	2.7
U						0.05		0.04	0.07	0.03					0.5	0.6	0.5	1.0
Reference	Stakes and Taylor, 2003	Stakes and Taylor, 2003	Stakes and Taylor, 2003	Stakes and Taylor, 2003	Stakes and Taylor, 2003	a	Stakes and Taylor, 2003	a	a	a	N. Christenson Unpubl.	Kurth et al. (1998)	Köksal et al. (2010)	Köksal et al. (2010)	Zhang et al. (2007)	Jiang et al. (2008)	Jiang et al. (2008)	Wanless et al. (2010)

[a] Data collected by combined XRF and ICP-MS at the University of Alabama.

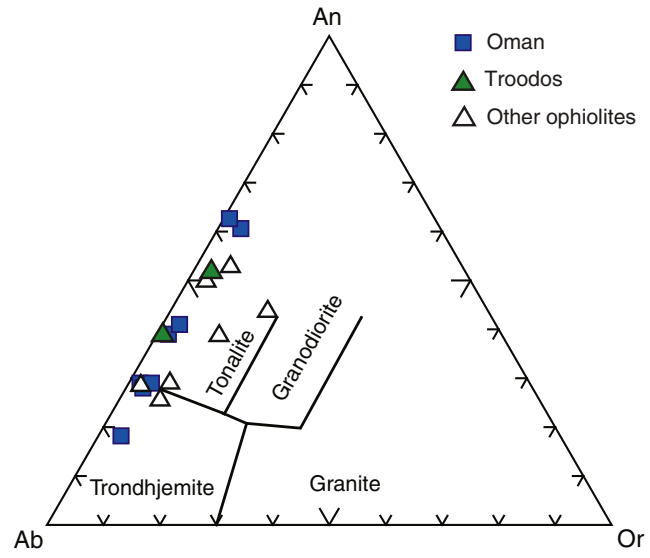

Fig. 2. Normative albite (Ab)–anorthite (An)–orthoclase (Or) contents for felsic rocks from ophiolites. The An–Ab–Or ternary is after Barker (1979).

for both fractionation of the existing melt lens and hydrous melting, promoting formation of evolved melts.

Large-scale plagiogranite intrusions in the northern part of Oman have been studied previously by several investigators (France et al., 2010; Lippard et al., 1986; Pallister and Knight, 1981; Rollinson, 2009; Stakes and Taylor, 1992, 2003). Lippard et al. (1986) and Stakes and Taylor (1992, 2003) described two main types. Most striking are the large (up to 8 km in areal extent) composite intrusions such as those

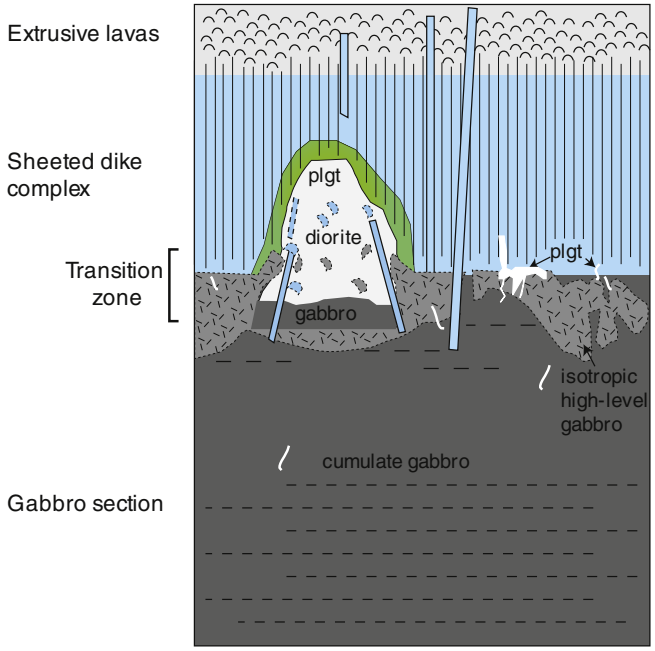

Fig. 3. Schematic cross-section of ocean crust showing plagiogranite intrusions occupying the dike-gabbro transition zone of an ophiolite (modified from Stakes and Taylor, 2003). The large plagiogranite body on the left depicts a 'late intrusive complex' (nomenclature of Lippard et al., 1986) intruding upper gabbro and the base of the sheeted dikes; these incorporate abundant xenoliths of mafic crust and may be cut by basaltic dikes. Low-$\delta^{18}O$ (WR) values are common in the surrounding country rock, and the upper contacts are hydrothermally altered to epidote- and chlorite-rich assemblages (shown as an aureole around the intrusion). The plagiogranites on the right depict smaller scale sheets/pods and thin (cm- to m-scale) dikes that intrude the upper isotropic gabbros and root zone of the sheeted dike complex. Plgt = plagiogranite.

from the Shafan, Aarja, and Suhaylay areas (Fig. 1; Appendix A). These intrusions were first described by Lippard et al. (1986) as 'late intrusive complexes' and interpreted to form via crystal fractionation within a high level magma chamber. The larger complexes are characteristically internally-zoned to more mafic rock types (diorite, gabbro), contain abundant xenoliths with signs of recrystallization (i.e., granoblastic textures) and/or partial digestion, and may be cut by multiple generations of basaltic dikes. Stakes and Taylor (2003) describe a metamorphic aureole around the large intrusions, characterized by hydrothermally altered wall rocks containing actinolitic hornblende, sodic plagioclase, epidote and titanite. A survey of isotopic data from diabase dikes, hydrothermal veins, and gabbroic rocks proximal to the large plagiogranite intrusions reveals that $\delta^{18}O$(WR) values typically vary between 4 to 12‰ (Stakes and Taylor, 2003; their Fig. 10). The $\delta^{18}O$(quartz) values span a narrower range of 4.1 to 8.2‰. Rare whole-rock $\delta^{18}O$ values extending down to +2‰ are observed in some areas, most notably around the intrusion near Wadi Shafan. Stakes and Taylor (2003) concluded that the large plagiogranite intrusions formed through extreme-open system processes involving 'assimilation of partially melted, hydrothermally-altered wall rocks and dikes, together with recharge by contemporaneous mafic dikes and limited fractional crystallization'. These conclusions were based on the field relations as well as non-MORB-like stable isotope systematics in quartz. In contrast, Rollinson (2009) examined an additional 'late intrusive complex' from the Oman ophiolite at Jebbel Fayyad (north of the Wadi Shafan area) in detail, and based on REE systematics concluded that it formed by fractional crystallization of a mafic parent derived from highly depleted mantle. The majority of samples in this study are from large-scale plagiogranite intrusions.

A second type of plagiogranite at Oman described by Stakes and Taylor (2003) occurs as cm-scale 'segregation dikes' that intrude high-level amphibole-bearing gabbros ('high-level intrusives', following the nomenclature of Lippard et al., 1986) emplaced early during the main stage of ophiolite construction. These smaller plagiogranite bodies are similar in scale to plagiogranite recovered along modern mid-ocean ridges (e.g., Grimes et al., 2011a; Koepke et al., 2007; Niu et al., 2002). Examples in this study include the plagiogranite from the Lasail (OM85-519a) and Musafiyah (OM81-25) areas (Table 1). In some cases, thin plagiogranite dikes reportedly coalesce up section to form thick sheet-like bodies, such as plagiogranite bodies near Rajmi (Stakes and Taylor, 2003). Stakes and Taylor (2003) and Rollinson (2009) both concluded that plagiogranite associated with the 'high-level gabbros' formed as the result of anatexis of hydrated gabbro.

3. Techniques

3.1. Analytical methods

In this study, zircon grains from 22 rock samples from 8 ophiolites have been analyzed for $\delta^{18}O$ values using SIMS (Table 3; Supplemental Table S1, S2). Additional zircons (12 spots) were analyzed from a dacite sampled at ~9°N, East Pacific Rise. Individual grains were separated from chips and hand samples either by mechanical crushing followed by a single density separation step using diiodomethane, or by dissolving the host rock in cold hydrofluoric acid, which assured complete recovery when available sample volumes were less than 100 g. Representative zircon grains were then hand-picked and cast in epoxy along with the oxygen isotope zircon standard KIM-5. Mount surfaces were flattened and polished to minimize surface topography across the area to be analyzed following the procedure described by Grimes et al. (2011a). All grains were imaged prior to analysis using SEM cathodoluminescence and backscattered electrons to evaluate zoning patterns and locate mineral inclusions and cracks. Oxygen isotope ratios were measured *in situ* at the University of Wisconsin-Madison SIMS laboratory (WiscSIMS) using a Cameca IMS-1280 during 4 separate sessions. Measurements were made with a focused Cs^+ beam with an intensity of 1.9–2.2 nA and a

Table 3
Summary of $\delta^{18}O$ values for magmatic zircon, quartz, and whole rock from ophiolite plagiogranite.

		$\delta^{18}O$ (‰, VSMOW)						Whole rock[a]	Quartz[a]
		Zircon							
		Ave.	2 SD	Min	Max	# grains	# spots		
Oman Ophiolite									
Rajmi									
1	OM81-75	4.9	0.5	4.7	5.1	3	3	6.2	
Suhaylay									
2	OM81-80	4.5		4.3	4.8	2	2	10.2	6.9
3	OM81-83	4.4	0.3	4.3	4.6	4	4		6.7
Aarja									
4	OM85-412	4.4	0.5	4.0	4.7	7	8	9.8	7.7
5	OM85-411	5.0	0.3	4.8	5.2	9	10	5.0	
Shafan									
6	OM81-153	4.7	0.5	4.3	5.1	12	14		
7	OM81-155	4.9	0.3	4.7	5.2	8	10		4.8[b]
8	OM81-156	4.8	0.1	4.7	4.9	6	6		5.3[b]
9	OM81-165	4.9	0.5	4.3	5.3	16	19	8.1	
Lasail									
10	OM85-519a	4.4	0.6	3.9	4.7	6	6	11.3	
Musafiya									
11	OM81-25	4.3	0.4	4.0	4.6	10	14	8.3	7.7
Troodos Ophiolite									
12	CG10-CY11	5.06	0.47	4.8	5.5	17	22		
13	CG10-CY3	5.06	0.46	4.7	5.5	19	24		
Fidalgo Island									
14	ML-8	4.96	0.26	4.8	5.2	10	18		
15	ML-3	5.06	0.49	4.5	5.4	12	16		
Western Lewis Hills, Bay of Islands									
16	WLH-22	5.01	0.26	4.8	5.2	13	19		
Ekecikdag									
17	EK-40	4.8	0.31	4.6	4.9	7	8		
18	EK-41	4.88	0.39	4.6	5.2	7	7		
Canyon Mountain									
19	CM-05-1	4.78	0.16	4.6	5.0	10	10		
Lagkor Lake									
20	G1011 GZ-1	4.94	0.31	4.8	5.1	12	12		
Oytag									
21	WYT-5 magmatic	4.66	0.33	4.5	4.9	6	6		
	inherited	6.73	0.89	6.4	8.4	6	8		
22	GZ-1	4.92	0.77	4.5	5.6	6	6		
9°N, EPR dacite									
23	265–70	4.8	0.3	4.6	5.0	8	12	6.1	

[a] Laser fluorination data reported by Stakes and Taylor (2003).
[b] Quartz aliquots analyzed at the Univeristy of Wisconsin-Madison stable isotope facility by CO_2 laser fluorination following methods described by Spicuzza et al. (1998); data were corrected to the Gore Mountain garnet standard UWG-2 (5.80‰).

spot size of ~10 μm in diameter and 1 μm deep following the methods described by Kita et al. (2009). Four analyses of the standard were performed routinely at the beginning of each session, and subsequently after every 10–12 unknowns. The bracketing analyses on KIM-5 ($\delta^{18}O = 5.09$ VSMOW, Valley, 2003) were used to correct for instrumental mass fractionation. The spot-to-spot reproducibility (external precision) for individual brackets of KIM-5 averaged 0.24‰ (2 standard deviations, SD) during these sessions. Following analyses, all ion microprobe pits were reexamined by SEM and classified based on pit shape and the presence of any irregular textures or mineral inclusions.

Quartz was hand-picked from samples OM81-155 and OM81-156 and analyzed by CO_2-laser fluorination analysis (BrF_5) at the University of Wisconsin-Madison following the methods described by Valley et al. (1995) and Spicuzza et al. (1998). Measurements were standardized with 4–5 analyses of UWG-2 garnet standard ($\delta^{18}O = 5.8$‰; Valley et al., 1995), and are reported in standard δ-notation relative to Standard Mean Ocean Water (SMOW). These data are combined with published data from Stakes and Taylor (1992, 2003) in Table 3.

3.2. Zircon textures revealed by SEM

Cathodoluminescence imaging of zircons from ophiolite plagiogranite show textures and zoning patterns comparable to those reported for zircons from modern mid-ocean ridge crust (Grimes et al., 2009; Schwartz et al., 2010). The vast majority of grains examined show well-developed oscillatory and/or sector zoning (Fig. 4; Online Supplemental Fig. S1) attributed to magmatic growth (e.g., Corfu et al., 2003). Grains targeted for analysis were typically clear and colorless in plane light. Rare rim overgrowths with distinctive bright CL were noted on four grains in Oman sample OM81-153. An additional textural type of zircon is common in samples from the Oman and Troodos ophiolites. These grains appear milky white, pink, or yellow in plane light, are characterized by patchy/chaotic, non-concentric zonation, and contain micron to submicron-scale inclusions or voids. Within single grains, inclusion-rich domains with irregular zoning may truncate domains with oscillatory zoning. Zircons with similar textures are described from ophiolites and young (<2 Ma) mid-ocean ridge crust, and have been interpreted by Schwartz et al. (2010) to form by secondary alteration involving fluid-assisted dissolution–reprecipitation reactions. Exploratory $\delta^{18}O$ analyses were carried out on 32 zircons (55 spots) from 7 rocks to characterize these inclusion-rich domains, but caution is urged when interpreting the measured $\delta^{18}O$ values. Post-SIMS imaging commonly reveals open pores in the bottom of pits within these domains, which may have been fluid inclusions. These domains do not preserve primary igneous textures, and measured values may reflect mixing of primary & secondary zircon, as well as inclusions.

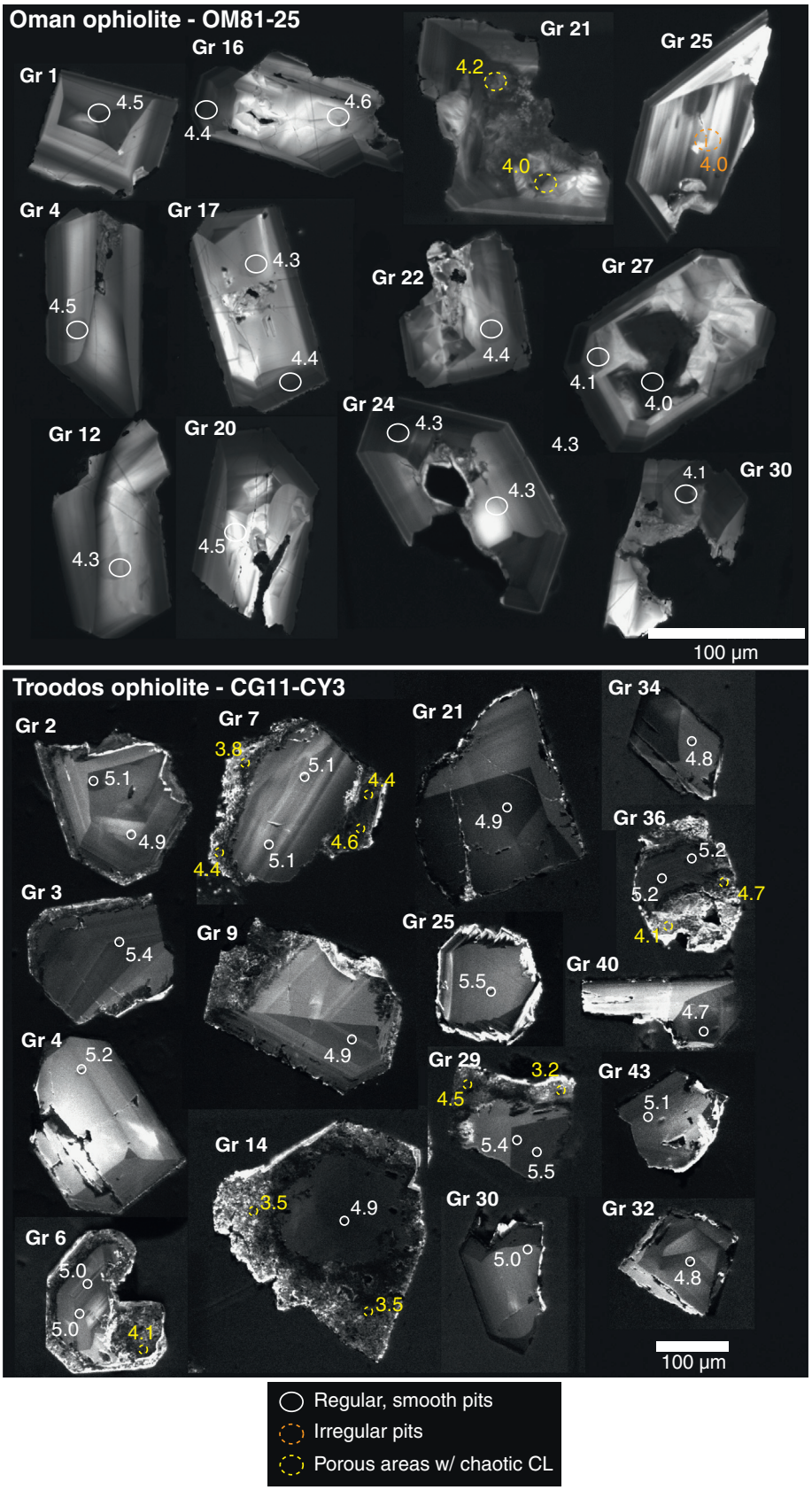

Fig. 4. Representative cathodoluminescence images for zircon hosted by plagiogranite from the Oman and Troodos ophiolites. Zircon grains are commonly oscillatory and/or sector zoned, consistent with magmatic growth. Secondary domains characterized by a lack of regular zonation and dense inclusions occur within some grains (e.g., CG11-CY3 Gr 6, 9, 14 and 36). Circles indicate the location of ion microprobe analysis spots; $\delta^{18}O$ values are listed beside each spot (‰, VSMOW). Analysis spots on normal, magmatically zoned domains are shown with solid lines; analysis spots on irregular zircon domains are shown as dashed circles, and were rejected following post-SIMS analysis SEM imaging. Additional images are provided in Online Supplemental Fig. S1.

Table 4
Summary of SIMS δ18O spots on porous, inclusion-rich zircon and rare late rims.

		δ^{18}O (‰, VSMOW)			
		Min	Max	# Grains	# Spots
Oman					
1	OM81-75	2.3	4.7	7	11
4	OM85-412	2.9	4.5	7	11
6	OM81-25	4.0	4.2	1	2
7	OM81-153 porous	3.4	–	1	1
	Rims	0.1	3.2	4	7
11	OM85-519a	2.1	4.2	7	12
Troodos, Cyprus					
12	CG10-CY11	1.7	4.1	4	7
13	CG10-CY3	3.2	4.7	5	11

Following SEM imaging of analysis pits, ~4% (15 out of 279 spots) of analyses on zircon with magmatic textures were rejected on the basis that they overlapped cracks or inclusions, although including them does not modify the measured δ^{18}O range. An additional 62 spots intentionally placed on inferred non-igneous textural domains (i.e., inclusion-rich grains with irregular zoning, bright CL rims) are reported separately, and are summarized in Table 4. All analyses are listed by sample in the Online Supplemental Table S1, and in analytical sequence with analytical standards in Online Supplemental Table S2.

4. Results

Zircon from ophiolites exhibit magmatic δ^{18}O(Zrn) values that are consistently at or mildly below δ^{18}O(Zrn) in high-temperature equilibrium with uncontaminated MORB (5.3 ± 0.6‰ (2SD); Valley et al., 2005) (Figs. 5; 6). The average δ^{18}O of all ophiolite plagiogranite-hosted zircon cores free of cracks and inclusions is 4.9 ± 0.6‰, which is mildly depressed compared to MORB-like values measured on zircons occupying deeper gabbroic sections of slow-spreading oceanic crust (5.2 ± 0.5‰; Grimes et al., 2011a). Comparison of the population of δ^{18}O(Zrn) values from ophiolites with those from slow-spreading ocean crust using a Student's *t*-test indicates a significant difference in the sample means at >99.9% confidence ($p = \ll 0.001$). Dacite sampled from 9°N along the East Pacific Rise yields δ^{18}O(Zrn) of 4.6–5.0‰ (rock average = 4.8‰), falling at the low end of the mantle-like range. Magmatic zircon from individual rocks typically exhibit ranges in δ^{18}O of 1‰ or less, and magmatic domains in single grains are typically uniform at the level of analytical precision. The only exception involves rare rims analyzed on four grains from Oman sample OM81-153, which extend to δ^{18}O values of 0.1‰ and are up to ~5‰ lower than oscillatory-zoned magmatic cores within the same grains.

Plagiogranite sampled from the Oman ophiolite extend to the lowest magmatic δ^{18}O values (Fig. 6), with individual spots on magmatic zircon ranging from 3.9 to 5.3‰. Individual zircon from 5 of the 6 intrusions sampled give δ^{18}O values below the mantle-like range (Fig. 5). The intrusion near Rajmi (OM81-75) contained exclusively mantle-like δ^{18}O, but only 3 grains with magmatic textures were analyzed. Individual intrusive bodies can be heterogeneous, as in the case of the Aarja plagiogranite body (OM85-412, 411 with sample-average δ^{18}O = 4.4 and 5.0‰, respectively), or quite uniform as observed for the body near Shafan (four rocks with average δ^{18}O = 4.7 to 4.9‰). No systematic variation in δ^{18}O from north to south, or plagiogranite size is observed. The lowest δ^{18}O(Zrn) values observed are found both in the km-scale, late-stage intrusions and the cm-scale segregation dikes that intrude high-level intrusive gabbros formed during the main stage of ophiolite construction (Fig. 6). For example, the thin plagiogranite dikes from Musafiyah (OM81-25) and Lasail (OM85-519a) in central and northern Oman give sample-average δ^{18}O(Zrn) values of 4.4 and 4.3‰, respectively. The 8 × 10 km-wide composite intrusion near Suhaylay (OM81-80, 83) is an example of a 'late intrusive complex' identified by Lippard et al. (1986), and has δ^{18}O(Zrn) of ~4.4‰. All spots on magmatic zircon from the Oman ophiolite give an average δ^{18}O(Zrn) of 4.7 ± 0.7‰. The δ^{18}O(Zrn) of ophiolites other than Oman define a narrower range and have a higher average value of 5.0 ± 0.4‰, which is not distinct from mantle-like values.

Within the volcanic-arc-type Oytag ophiolite (northwest China, sample WYT-5), a population of older inherited zircons were previously identified (Jiang et al., 2008) based on Pb/U age and εHf values. SHRIMP Pb/U ages reveal a younger population with a weighted mean age of 327.7 ± 4.9 Ma, and older grains ranging from 435 to 480 Ma and notably higher uranium concentration. The younger grains have MORB-like εHf values of 13.7 to 19.5, whereas the older grains range from −1.9 to +3.1 epsilon units. The older suite of zircon is reportedly similar to Ordovician granitoids exposed in the region, and were interpreted as xenocrysts incorporated during formation of the Oytag Ophiolite in an island arc setting (Jiang et al., 2008). Oxygen isotope ratios measured on the older population average 6.7‰, consistent with inheritance from a continental granitic source. The younger population is interpreted by Jiang et al. (2008) to have crystallized directly from the plagiogranite magma, and has an average δ^{18}O = 4.7‰.

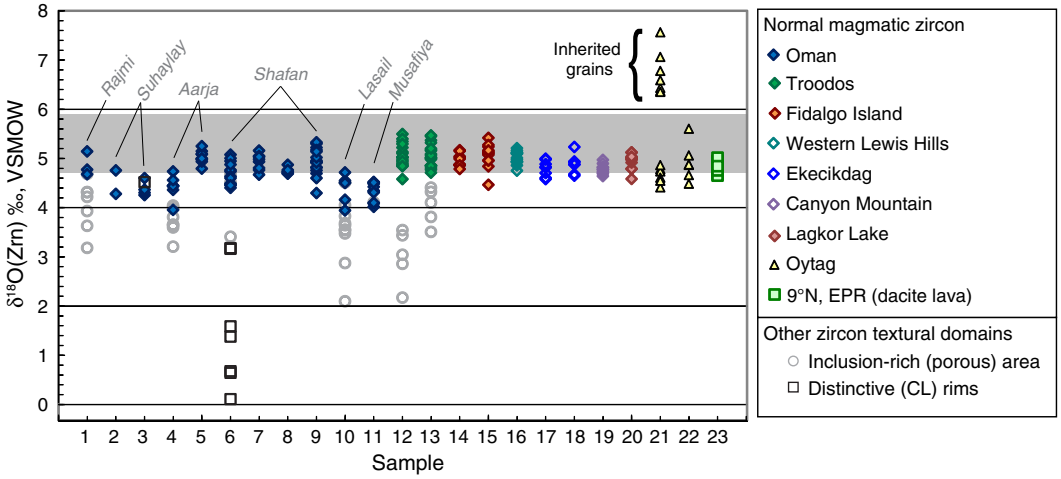

Fig. 5. Measured δ^{18}O for zircons from silicic magmas sampled from various ophiolites and the East Pacific Rise. Each data point represents a single grain, unless noted otherwise (e.g., rims, cores). Sample numbers along the x-axis correspond to those listed in Table 1. Normal magmatic domains were typically homogeneous within single crystals at the level of analytical uncertainty (better than ±0.3‰, 2SD). The shaded horizontal bar represents δ^{18}O(Zrn) values in high-temperature equilibrium with mantle (5.3 ± 0.6‰, 2 SD; Valley et al., 1998, 2005). Inherited zircons from the Oytag Ophiolite were identified on the basis of Pb/U age and εHf value, and have been interpreted to originate from contamination by sediment during construction of this ophiolite within an island arc setting (i.e., Jiang et al., 2008); the inherited grains are therefore not representative of the plagiogranite δ^{18}O(magma).

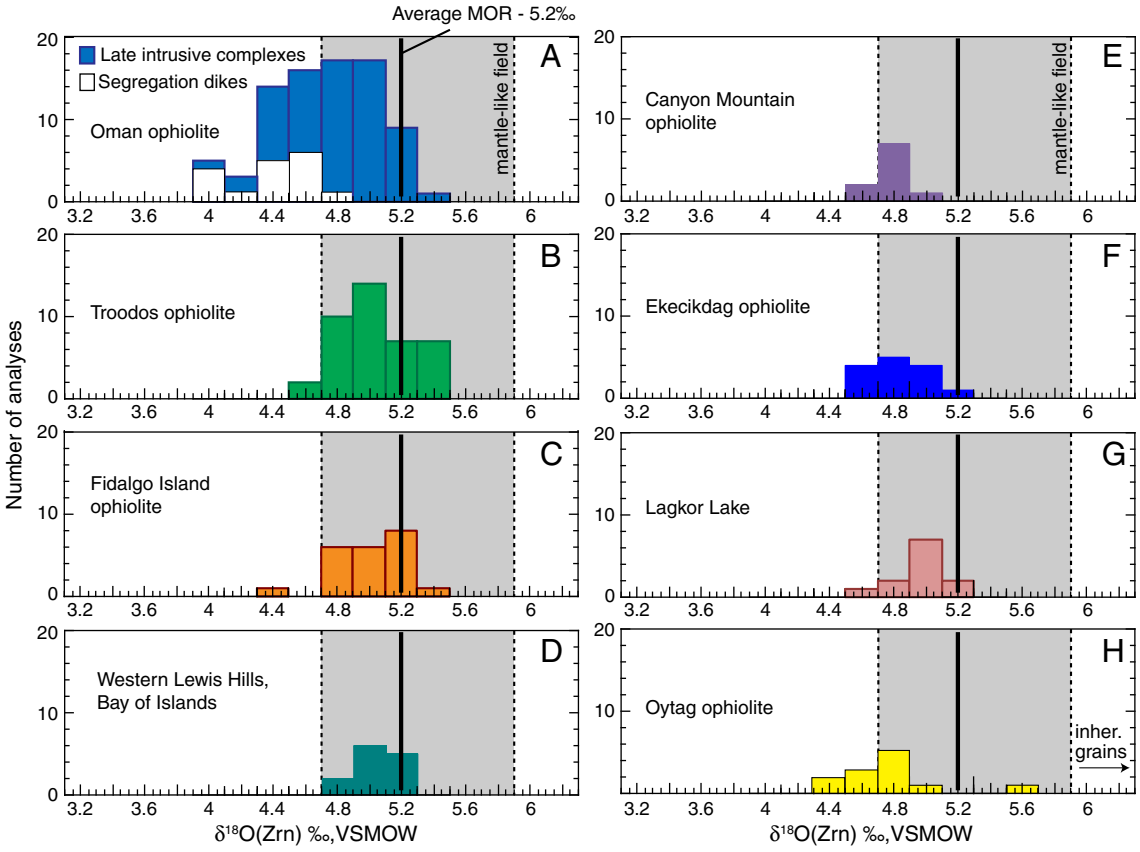

Fig. 6. Histograms comparing $\delta^{18}O$(Zrn) of plagiogranite from the ophiolites surveyed. The shaded vertical bar represents $\delta^{18}O$(Zrn) values in high-temperature equilibrium with the mantle; the dashed vertical line at 5.2‰ indicates the average $\delta^{18}O$ of zircons from gabbroic crust formed at modern slow spreading mid-ocean ridge environments (Grimes et al., 2011a).

Measured $\delta^{18}O$ values below 3.9‰ are exclusively from inclusion-rich, texturally-chaotic zircon domains, and the rare rims mentioned previously (Fig. 5). These domains appear to post-date igneous crystallization of zircon from the silicic magmas based on the observed textures. The low-$\delta^{18}O$ rims (measured on only 4 grains) are up to ~5‰ lower than oscillatory-zoned magmatic cores within the same grain, implying either crystallization from later, low $\delta^{18}O$ magma previously unrecognized in this setting, or precipitation from an aqueous fluid. Cavosie et al. (2009) calculated that zircon precipitated from hydrothermal fluids ($\delta^{18}O_{(H2O)} \approx 2$‰) could have $\delta^{18}O$(Zrn) values near 0‰. In the absence of any additional evidence for such low- $\delta^{18}O$ magmas in this setting, a hydrothermal origin is favored for the rare rims although further investigation will be required to evaluate this hypothesis further. The inclusion-rich, texturally-chaotic zircons found in samples from the Oman and Troodos ophiolites yield variable $\delta^{18}O$ from 1.7 to 4.7‰. The irregularly-zoned zircon domains are heterogeneous in $\delta^{18}O$ (up to 3‰ range in a single rock), and may reflect partial resetting of preexisting igneous domains. These domains are not interpreted as igneous; their origin is beyond the scope of the current study and will be considered further elsewhere.

5. Discussion

5.1. $\delta^{18}O$ of magmatic zircon from ocean crustal settings

Previous oxygen isotope studies of zircons from modern mid-ocean ridge environments are limited to rocks collected from fracture zones and oceanic core complexes, where gabbroic crust and mantle peridotite have been exposed to the seafloor by tectonic denudation (e.g., Cavosie et al., 2009; Grimes et al., 2011a). The $\delta^{18}O$(Zrn) values of those mid-ocean ridge plagiogranite are indistinguishable from $\delta^{18}O$(Zrn) of fractionated Fe–Ti oxide gabbro; both are exclusively MORB-like (5.2 ± 0.5‰; 2 SD), plotting entirely within the restricted mantle-like $\delta^{18}O$ range of 5.3 ± 0.6‰ (2SD). The absence of a seawater signature was interpreted to indicate either that the plagiogranite magma formed by closed-system fractional crystallization of a mantle-derived melt, or by remelting of crust prior to detectable modification of the protolith $\delta^{18}O$. The range of $\delta^{18}O$ recorded by the magmatic ophiolite zircon reported here is also fairly restricted (3.9–5.6‰), but ~0.4‰ lower on-average than the mantle-like value and typical zircon in lower gabbroic crust sampled along modern slow-spreading mid-ocean ridges (Fig. 7). Grimes et al. (2011a) modeled the effect of temperature and varying parent melt composition on the value of $\delta^{18}O$(Zrn) during closed-system fractionation of a parent with MORB-like $\delta^{18}O$(WR), and demonstrated that zircon values down to ~4.7‰ could result if crystallization occurred below ~700 °C from parental melts with >70 wt.% SiO_2. Small volumes of contamination by partial melting of crust that experienced only mild shifts in $\delta^{18}O$ (~<0.5‰) during water–rock interaction, or melting of fortuitous mixtures of both high- and low-$\delta^{18}O$ crust could also produce magmas with $\delta^{18}O$ values in the narrow mantle-like range and cannot be distinguished on the basis of oxygen isotopes alone. However, low $\delta^{18}O$(Zrn) values <4.7‰ or high $\delta^{18}O$ values >5.9‰ are a clear indication of magma interactions with hydrothermally altered crust. Therefore, the low $\delta^{18}O$ values below 4.7‰ observed in many plagiogranites from the Oman ophiolite, and the Oytag ophiolite (which contains inherited zircons) must have formed by remelting of crust modified to lower $\delta^{18}O$ by high-temperature hydrothermal alteration.

Other ophiolites yield $\delta^{18}O$ values within the mantle-like range (rock average $\delta^{18}O$ = 4.7–5.1‰), making their mode of origin ambiguous based on $\delta^{18}O$ alone. However, it is noteworthy that rock-averaged $\delta^{18}O$ values from all sample locations are below the average mantle-like value of 5.3‰, and only 17 out of 256 spots on magmatic grains (excluding inherited grains from Oytag) gave $\delta^{18}O$ values of 5.3‰ or higher

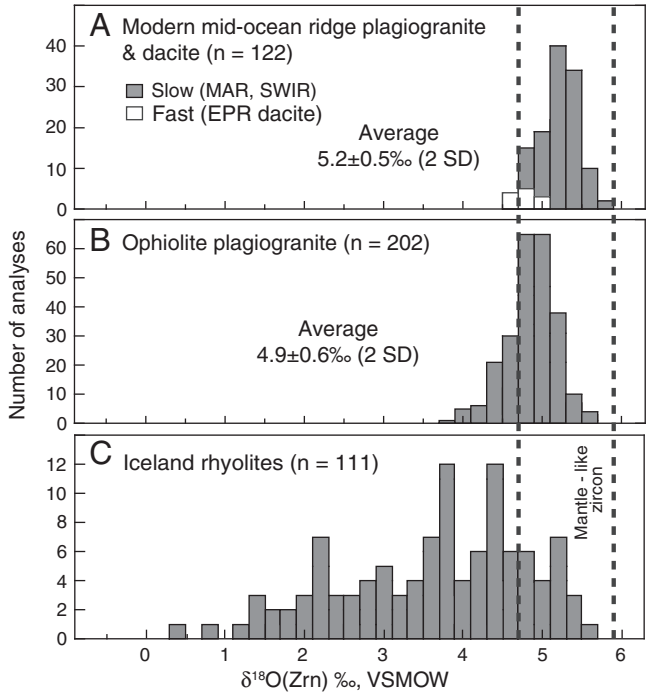

Fig. 7. Histograms comparing $\delta^{18}O$(Zrn) from A) plagiogranite-hosted zircons from the slow spreading Mid-Atlantic and SW Indian Ridges (Grimes et al., 2011a), B) ophiolite plagiogranite (this study; excluding inherited cores from the Oytag ophiolite), and C) Iceland rhyolite (Bindeman et al., 2012).

(Fig. 6). The systematic shift relative to average mantle-like values indicates that contamination by hydrothermally-altered crust may be a common phenomenon in the ophiolites surveyed, and that melting/contamination is dominated by crust modified to low-$\delta^{18}O$ values. In typical ocean crust, low $\delta^{18}O$ values develop during interactions with seawater-derived fluids at temperatures above ~300 °C and are characteristically observed near the base of the sheeted dike complex and in the upper gabbros (Fig. 8).

Considerably lower-$\delta^{18}O$ silicic lavas are reported at Iceland. Bindeman et al. (2012) measured $\delta^{18}O$(Zrn) values down to ~1‰ in Icelandic rhyolite lavas (Fig. 7c), and concluded that remelting of hydrothermally altered crust was an important factor in their formation. Icelandic crust differs from typical mid-ocean ridge and ophiolite settings in that it is thicker, and exposed subaerially due to involvement of the hot spot plume. The measured magmatic $\delta^{18}O$(Zrn) values reflect $\delta^{18}O$ of the Icelandic crust available for remelting (−12 to +4‰; Hattori and Muehlenbachs, 1982; Gautason and Muehlenbachs, 1998), which arises from interactions with high-latitude meteoric waters that are much lower in $\delta^{18}O$ than seawater ($\delta^{18}O$ = 0‰).

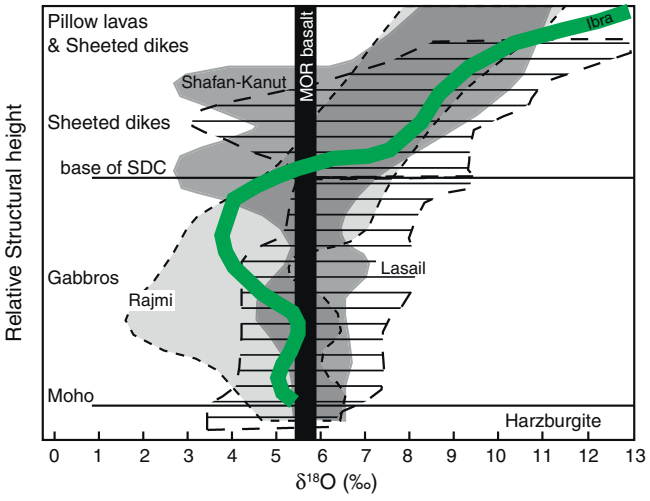

Fig. 8. Whole rock $\delta^{18}O$ versus depth profiles reported for several transects throughout the northern Oman ophiolite (data from Stakes and Taylor, 1992, 2003). Following Stakes and Taylor (2003) the profiles are arranged with depth in a qualitative fashion, relative to primary ophiolite stratigraphy. The generalized $\delta^{18}O$ profile of the Ibra section of Oman (Gregory and Taylor, 1981) is shown for comparison (bold curve). Vertical black bar illustrates the $\delta^{18}O$ of unaltered MORB. SDC = sheeted dike complex.

5.2. Petrogenesis of ophiolite plagiogranite: geochemical constraints

A characteristic compositional feature identified in experimental partial melts of hydrated gabbro and diabase is low TiO_2 concentration (<~1 wt.% at SiO_2(WR) > ~55 wt.%), which has been proposed as a diagnostic indicator of natural plagiogranite formed through partial melting of mafic ocean crust (France et al., 2010; Koepke et al., 2007). The felsic rocks investigated here contain TiO_2 concentrations both above and below the limit for experimental MORB fractionation (Fig. 9A), and on the ternary TiO_2–K_2O–SiO_2/50 diagram proposed by France et al. (2010), plagiogranite from the Oman ophiolite overlap experimental melts formed though both fractional crystallization and hydrous partial melting of mafic ocean crust (Fig. 9B). Of the Oman samples above the TiO_2-limit for fractional crystallization on Fig. 9A, only 1 (OM81-75) has $\delta^{18}O$(Zrn) values that are mantle-like. Within the suite of ophiolite plagiogranite investigated, values of $\delta^{18}O$(Zrn) are not obviously correlated with TiO_2(WR), but considering both TiO_2(WR) and $\delta^{18}O$(Zrn) from the same rocks (Fig. 9C) reinforces the interpretation that most of these rocks could not have formed through differentiation of MORB in a closed system.

In addition to TiO_2, Brophy (2009) presented modeling evidence that SiO_2 versus REE systematics should differ for melts formed by fractional crystallization and those formed by hydrous partial melting reactions. The behavior of REE is sensitive in large part to the presence of amphibole left behind in the residue, during hydrous partial melting involving a reaction such as olivine + Cpx + $Plag_{old}$ + H_2O = hornblende + Opx + $Plag_{new}$ + silicic melt (e.g., Koepke et al., 2007). Brophy (2009) demonstrated that fractional crystallization produces a positive correlation between concentrations of SiO_2 and La or Yb, whereas hydrous melting produces flat or even decreasing REE trends with increasing SiO_2 for plagiogranite and coexisting mafic crust. On a plot of La vs. SiO_2 (Fig. 10), published data for Oman plagiogranite and associated rocks define a flat trajectory consistent with an origin dominantly involving hydrous partial melting. Collectively, the minor, trace, and stable isotope geochemistry support an origin by hydrous partial melting and/or contamination of a fractionating melt lens for most of the plagiogranite sampled from the Oman ophiolite. The TiO_2 concentrations of plagiogranite from other ophiolites are also most consistent with an origin involving partial melting (Fig. 9C), although they commonly exhibit $\delta^{18}O$ values within the mantle-like range indicating that crust undergoing remelting was not detectably altered in $\delta^{18}O$.

As concluded by Rollinson (2009) from studies of field relations and REE characteristics of Oman plagiogranites, it is likely that both fractional crystallization of MORB and partial melting of hydrated crust occur to produce different plagiogranite intrusions. Brophy (2009) reached a similar conclusion for ophiolite plagiogranite and silicic volcanics in oceanic settings in general, and proposed the method using SiO_2 versus La or Yb to distinguish between the end-member processes. Hybrid processes are undoubtedly important (Wanless et al., 2010, 2011), though they may not always be evident from a single geochemical system. For example, Brophy (2009) concluded from REE vs. SiO_2 systematics of Icelandic rhyolite from the within-rift Torfajökull volcano (Fig. 10) that fractional crystallization was a dominant mechanism in their petrogenesis, while unambiguous evidence for remelting of hydrothermally altered crust comes from low-$\delta^{18}O$ values in glass and zircon phenocrysts (e.g., Bindeman et al., 2012; Hattori and Muehlenbachs, 1982). Additionally, Wanless et al. (2010, 2011) demonstrated that dacite

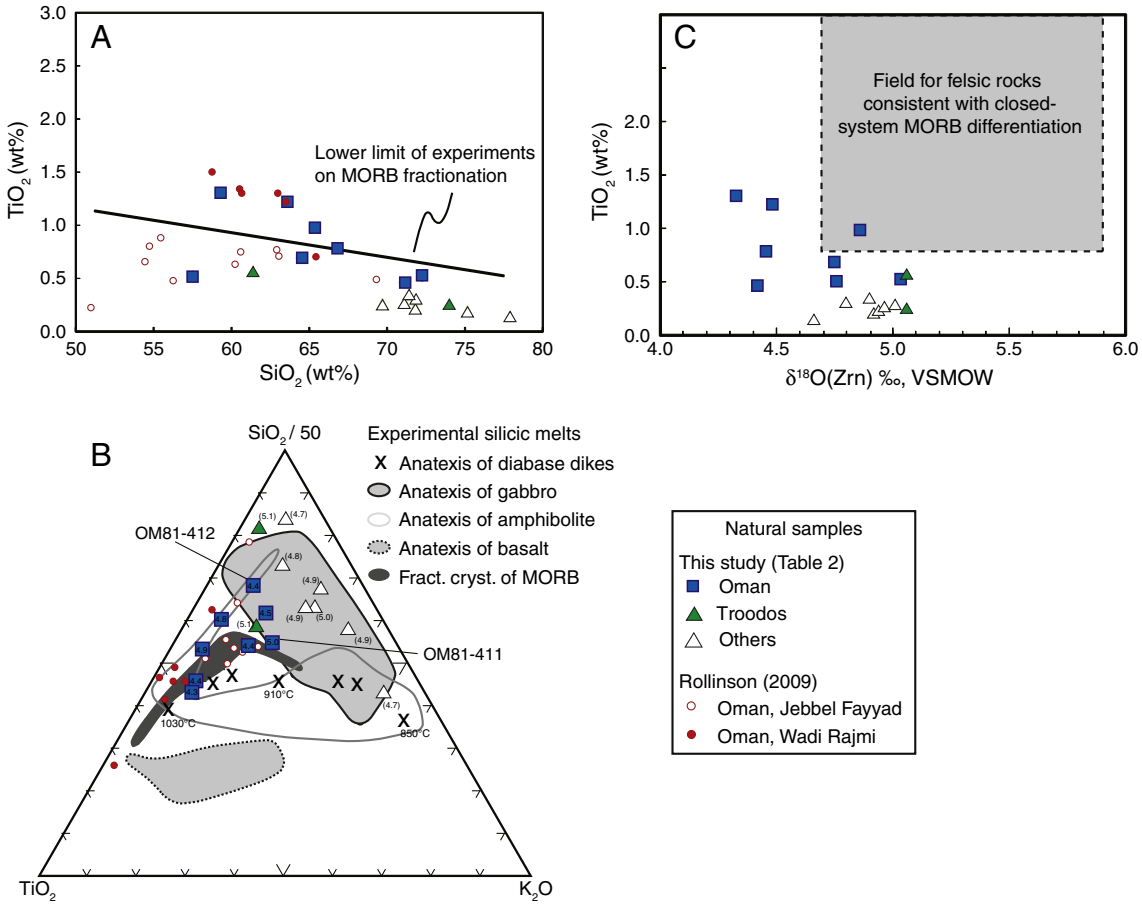

Fig. 9. Whole rock petrogenetic discrimination diagrams: A) TiO_2 versus SiO_2 (Koepke et al., 2007) and B) TiO_2–SiO_2/50-K_2O ternary (France et al., 2010), based on experiments involving hydrous melting of mafic ocean crust and fractional crystallization of mid-ocean ridge basalt (MORB). Natural plagiogranite surveyed are variable in composition, and overlap the fields for both fractional crystallization of MORB and partial melting of amphibole-bearing gabbro. Several of the natural samples overlapping the experimental field for MORB fractional crystallization exhibit low-$\delta^{18}O$(Zrn) values (rock-average values are listed in B with each data point), indicating that they could not have formed in a closed-system. The different fields displayed are from France et al. (2010) (diabase anatexis), Koepke et al. (2004) (gabbro anatexis), Beard and Lofgren (1991) (amphibolite anatexis), Thy et al. (1999) (basalt anatexis), and Dixon-Spulber and Rutherford (1983) and Berndt et al. (2005) (fractional crystallization of MORB). Data reported by Rollinson (2009) for natural plagiogranites from Jebbel Fayyad and Wadi Rajmi (Oman) are shown for comparison in A and B. C) TiO_2(WR) versus $\delta^{18}O$(Zrn) diagram showing the compositional field (shaded) for felsic rocks formed by differentiation of uncontaminated MORB.

lavas from the East Pacific Rise formed through combined assimilation/fractional crystallization processes using comprehensive geochemical modeling of elemental, volatile, and oxygen isotope geochemistry. Evidence for assimilation came mainly from volatile concentrations (elevated H_2O, Cl) and stable isotope values ($\delta^{18}O$) that are incompatible with fractional crystallization alone. Combining trace elements and stable isotopes is critical for evaluating contamination, particularly in oceanic settings where the existing crust available for contamination is otherwise quite similar to the composition of intruding magmas.

5.3. Remelting of hydrothermally altered crust near the dike-gabbro transition

The dike-gabbro transition in modern fast-spreading ocean crust and in ophiolites is often envisioned as the fossilized roof zone of a melt lens, where magmatic and hydrothermal systems interact and may overlap during active crustal accretion (e.g., France et al., 2009; Gillis, 2008; Gillis and Coogan, 2002; Nicolas et al., 2008) (Fig. 11A). Such a process may be common beneath magmatically-robust spreading centers, whether they occur in suprasubduction zones or fast-spreading mid-ocean ridge environments such as the East Pacific Rise. For the formation of plagiogranite within this horizon, we adopt the model described by France et al. (2010) in which hydrothermally-altered crust in the roof zone is reheated during upward migration of an underlying melt lens (Fig. 11B–C). As temperatures exceed ~850 °C, partial melting of stoped blocks and surrounding wall rock occurs, producing silicic melts that are then either assimilated, leading to contamination of MORB in the underlying melt lens, or intrude locally into the base of the sheeted dikes (France et al., 2013; Koepke et al., 2011). The volatile-enriched, contaminated melt may then continue to undergo crystal fractionation upon cooling.

The $\delta^{18}O$ of source rocks being melted and the extent of contamination may vary, as indicated by the pattern of $\delta^{18}O$-zonation observed in the plagiogranite intrusion near Aarja in the northern Oman ophiolite. A sample near the upper contact with the sheeted dikes (OM85-412) records low rock-averaged $\delta^{18}O$(Zrn) of 4.4‰ and SiO_2 content of 71 wt.%, with a major element composition broadly similar to experimental melts of hydrated diabase at ~900 °C (France et al., 2010) (Fig. 9B). In contrast, plagiogranite from the lower contact with gabbro (OM85-411) has a mantle-like $\delta^{18}O$(Zrn) of 5.0‰ and SiO_2 content of 58 wt.%. The high-level sample is consistent with melting of low-$\delta^{18}O$ crust near the roof of the melt lens, whereas formation of the deeper sample involved little or no contamination by a $\delta^{18}O$-modified source. Such zonation may be present in other large plagiogranite intrusions, but further sampling will be required to evaluate this hypothesis. As noted by France et al. (2010, 2013) and Koepke et al. (2011), contamination of the underlying melt lens will lead to an increase in SiO_2 content of the assimilating MORB magma, as well as K_2O, rare earth elements and chlorine. The elevated chlorine identified in MORB and erupted at fast spreading ridges and hornblende within upper gabbros from the Oman

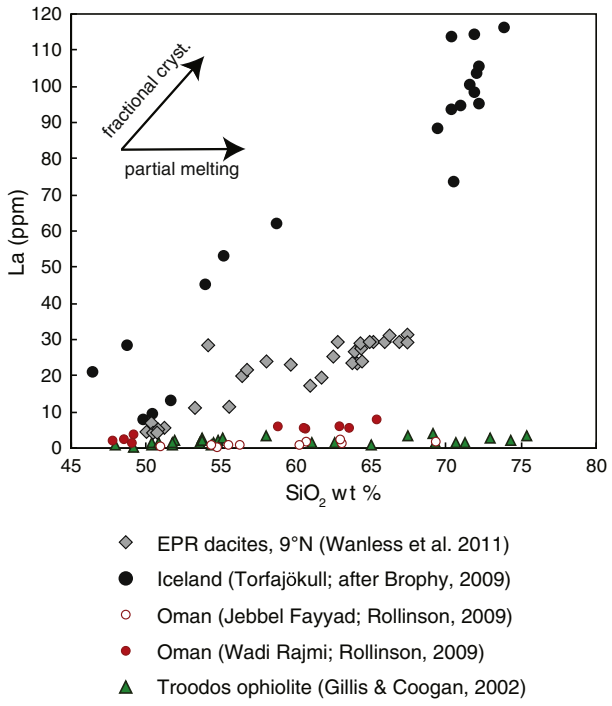

Fig. 10. La versus SiO_2 diagram proposed by Brophy (2009) for evaluating petrogenesis of silicic rocks in ocean crust. Conclusions from geochemical modeling indicate that silicic magmas formed through dominantly fractional crystallization show progressive enrichment in REE with increasing SiO_2, whereas melts formed by hydrous partial melting of mafic crust with hornblende left in the residue show flat or even decreasing REE concentration with increasing SiO_2. Rare earth element data for plagiogranite from the Oman ophiolite (Rollinson, 2009) and Troodos ophiolite (Gillis and Coogan, 2002) exhibit the flat trajectories characteristic of end-member partial melting. Dacite lavas from the axial valley of the East Pacific Rise, ~9°N, (Wanless et al., 2011) and rhyolite lavas from the Torfajökull volcano in Iceland (after Brophy, 2009) suggest the dominant process leading to their formation was fractional crystallization. However, constraints from stable isotopes and volatile concentration indicate that the lavas erupted at the East Pacific Rise and Torfajökull did not evolve in a closed system, and were heavily contaminated by hydrothermally altered components. Data for EPR dacite are from Wanless et al. (2011).

ophiolite (Coogan, 2003; Coogan et al., 2003; Michael and Schilling, 1989) is also the result of assimilation of hydrothermally altered crust. Shallow-level contamination of MORB within magmatically-robust spreading environments reflects the concurrent processes of magmatism and hydrothermal circulation in close proximity within the specialized, yet extremely widespread dike-gabbro transition zone.

5.4. $\delta^{18}O$ of plagiogranite magmas and constraints on the source rocks being melted

The classic profile of the oxygen isotope values from altered oceanic crust (Fig. 8) depicts $\delta^{18}O$ values from >+9‰ in the extrusive lavas, decreasing with depth through the sheeted dikes to values as low as ~+2‰, and then gradually returning to MORB-like values of 5–6‰ with depth through the gabbro section (e.g., Eiler, 2001; Gregory and Taylor, 1981). In detail, individual transects through the Oman ophiolite exhibit a significant degree of lateral variability (i.e., Stakes and Taylor, 1992, 2003), and near the dike-gabbro transition the observed $\delta^{18}O$ values extend both above and below fresh MORB values (Fig. 8). Elevated values below the dike-gabbro transition are characteristic of transects where intense fracturing and major shear zones are mapped (e.g., Wadi Rajmi transect, Shafan-Kanut transect) or the crust has been modified in part by late-stage intrusive complexes (e.g., Lasail transect). Stakes and Taylor (2003) interpret the elevated $\delta^{18}O$ values as the result of later, retrograde hydrothermal exchange proceeding at temperatures as low as ~150–200 °C. We find no evidence that the high-$\delta^{18}O$ rocks were melted to form plagiogranite. The comparatively

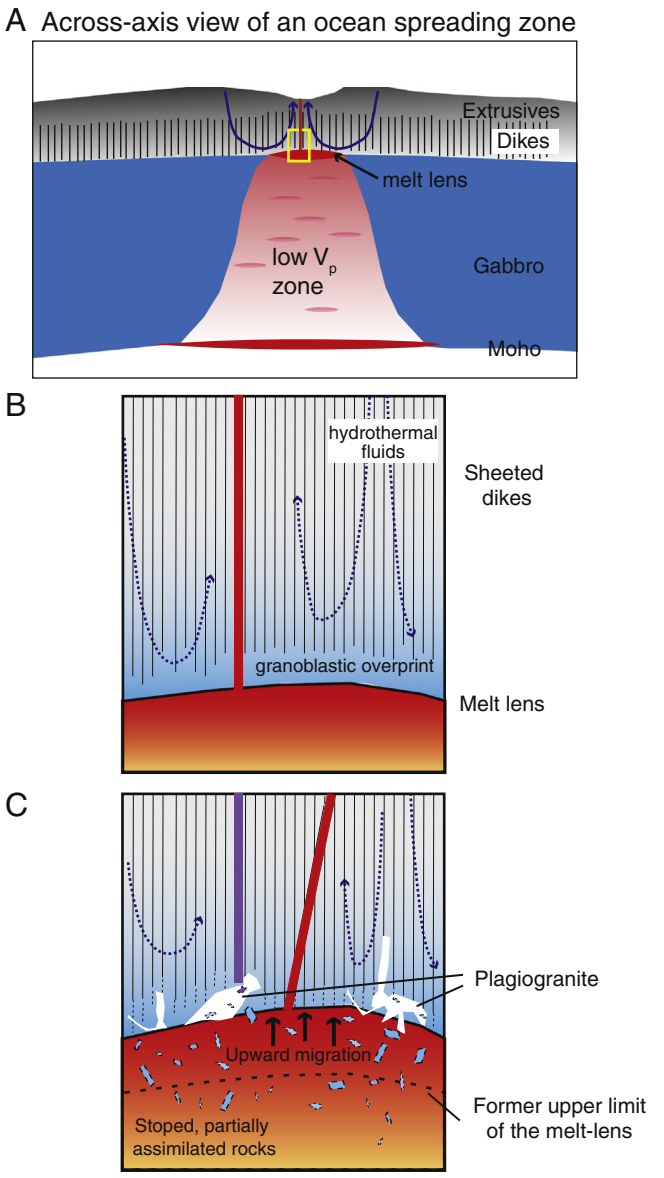

Fig. 11. Schematic depiction of the setting for plagiogranite formation near the dike-gabbro transition in magmatically robust spreading centers (modified after Gillis and Coogan, 2002; France et al., 2009). A) Simplified cross-section showing the structure of oceanic crust forming during extension. The yellow rectangle indicates the top of the axial melt lens. B) Closeup of the conductive boundary layer between an active melt lens and the overlying solidified dikes. This illustration depicts one stage of crustal accretion involving a steady state melt lens, and emplacement of dikes into the overlying crust. Hydrothermal fluids migrate downwards and interact to the basal zone of the sheeted dike complex. C) Vertical migration of the top of the melt lens due to replenishment results in recrystallization of the hydrothermally altered dikes, development of granoblastic textures, and hydrous partial melting to form plagiogranite (white), accompanied by assimilation and possibly partial melting of stope blocks leading to contamination of the melt lens.

mild-shifts to exclusively low $\delta^{18}O$ in plagiogranite magmas as seen from zircons vs. the large shift in variably altered whole rock values indicates that the magmas formed either by 1) partial melting and assimilation of variably modified, but generally low in $\delta^{18}O$, crust by an existing MORB-like magma, or 2) partial melting of crust following (or contemporaneous with) mild hydrothermal alteration at high temperature followed by segregation of the melt into surrounding country rocks. Field evidence for assimilation comes from the metamorphosed and partially resorbed xenoliths characteristic of late intrusive complexes at Oman (Coogan et al., 2003; France et al., 2009, 2013; Gillis, 2008; Stakes and Taylor, 2003). In either case, the consistently low $\delta^{18}O$ values characterized for the global suite of ophiolite plagiogranite

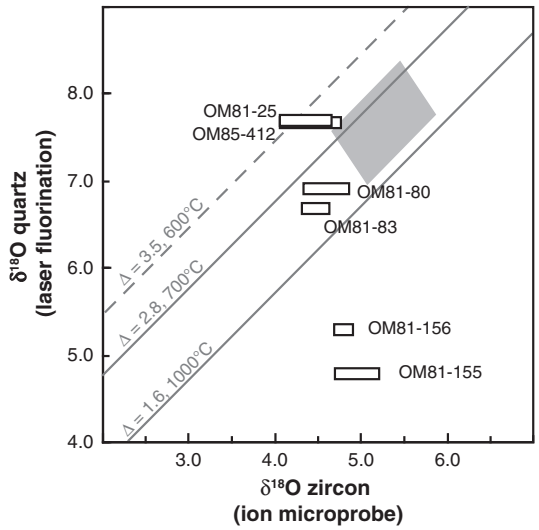

Fig. 12. $\delta^{18}O$(Zrn) versus $\delta^{18}O$(quartz) for coexisting mineral pairs in plagiogranite from the Oman ophiolite. Box widths depict the within-sample variation of $\delta^{18}O$ (zircon) determined from ion microprobe analysis. If the quartz-zircon pairs were in equilibrium at magmatic temperatures, they would define a linear array with a slope of 1. The subvertical array and widely varied fractionations shown indicate that the rocks have been hydrothermally altered and that quartz (measured by laser fluorination) has partially exchanged oxygen while the zircons preserve a narrow range of primary values. The solid diagonal lines encompass the range of magmatic fractionation between quartz and zircon at temperatures of 700–1000 °C. These were calculated using the fractionation factor reported by Valley et al. (2003); the conclusions do not change if the quartz-zircon fractionation factor of Trail et al. (2009) is used. The shaded gray box represents the approximate range of $\delta^{18}O$ expected for coexisting quartz and zircon in equilibrium with uncontaminated MORB.

indicate that melting and crystallization of ocean crust typically occurs prior to the later overprint by low-temperature (<250 °C) fluids. In the following section, we discuss the primary $\delta^{18}O$ values of plagiogranite magmas and possible constraints on assimilation from mass balance considerations.

The measured $\delta^{18}O$(WR) values for Oman ophiolite plagiogranite studied here range from 5.0 to 11.3‰ (Table 3), reflecting in large part, subsolidus alteration extending to low temperatures below ~250 °C. Stakes and Taylor (2003) calculated that the $\delta^{18}O$ of Oman plagiogranite magmas would have been approximately 4–7.5‰ on the basis of measured $\delta^{18}O$(quartz) values of 4.8–8.2‰, and noted that this range requires contamination by crust modified to both higher and lower $\delta^{18}O$ values. However, comparisons between $\delta^{18}O$ for quartz and zircon from the same rocks (Fig. 12) indicate that these minerals were not equilibrated at magmatic temperatures. The steep array defined by different quartz-zircon pairs in Fig. 12 indicates that quartz has been modified in most samples, and thus that there is no evidence for high $\delta^{18}O$ magmas at Oman.

An empirical calibration developed by Lackey et al. (2008) allows oxygen isotopic composition of a parental magma to be estimated from $\delta^{18}O$ of zircon and SiO_2 content of the magma. Under equilibrium conditions at magmatic temperatures, the oxygen isotopic fractionation between zircon and the host rock ($\Delta^{18}O$(Zrn-WR)) exhibits an approximately linear relationship with SiO_2 wt.%: $\Delta^{18}O(Zrn - WR) = \delta^{18}O(Zrn) - \delta^{18}O(WR) \approx -0.0612 * (wt.\%\ SiO_2) + 2.5$. Using this relation, the $\delta^{18}O$ of the Oman plagiogranite magmas are calculated to have been between 5.4 and 6.4‰, significantly less variable than estimates based on quartz and uniformly below $\delta^{18}O$ expected for evolved silicic magmas derived from uncontaminated MORB (Fig. 13A). Closed-system fractional crystallization of MORB ($\delta^{18}O$ ~ 5.6‰) would result in an increase in $\delta^{18}O$ of the magma by up to ~1–1.5‰ during the production of more silicic magmas (Muehlenbachs and Byerly, 1982; Wanless et al., 2011) (shown as a gray band in Fig. 13). Granoblastic dikes and gabbro with low-$\delta^{18}O$(WR) are reported around many large plagiogranite bodies of the northern Oman ophiolite, and represent a likely contaminant (Stakes and Taylor, 2003).

Interactions between seawater-derived fluids and ocean crust will rarely shift $\delta^{18}O$(WR) below 0–2‰, due to the small fractionation ($\Delta^{18}O$ ~ 0 to 1‰) between seawater and rocks at temperatures above ~400 °C. The lowest $\delta^{18}O$(WR) reported by Stakes and Taylor (2003) is ~2‰, measured on a mafic dike collected at the sheeted dike-high level gabbro contact near the Lasail plagiogranite. Assuming simple mixing of a contaminant with $\delta^{18}O(WR) = 2$ and a melt in $\delta^{18}O$-equilibrium with MORB, assimilated volumes of ~0–20% are required to produce the range of $\delta^{18}O$ values calculated for plagiogranite magmas (Fig. 13B). The calculated volume increases if a higher-$\delta^{18}O$-assimilant is assumed (Fig. 13C). These estimates are similar to the assimilated volume of hydrothermally altered crust required to explain chlorine concentrations and stable isotope ratios in basalt and dacite from the fast spreading East Pacific Rise (Coogan et al., 2003; Wanless et al., 2011).

The assimilation model considered above may be appropriate for the larger plagiogranite plutons in the root zone of the sheeted dikes of ophiolites, but it is implausible for the formation of cm-scale plagiogranite typical of plutonic crust exposed along slow-spreading ridges, or the 'segregation dikes' described by Stakes and Taylor (2003) from Oman. A somewhat different model proposed for plagiogranite genesis involves partial melting initiated by the ingress of seawater into still-hot, but solidified gabbros or dikes (Koepke et al., 2004, 2007). Koepke et al. (2007) estimated that as little as ~1 wt.% H_2O would be sufficient to produce ~10 wt.% of a felsic, water-saturated melt at pressures of 1–2 kbar provided temperatures exceed 850 °C. If the hydrating fluid were seawater ($\delta^{18}O = 0$), the modification in $\delta^{18}O$ by 1 wt.% H_2O would likely be too small to detect in the resultant partial melt (discussion by Grimes et al., 2011a). Thus, it would be possible for plagiogranite dikes throughout the crust to form by hydrous partial melting yet not carry a resolvable seawater-signature in $\delta^{18}O$. Since high water–rock ratios would also cool the rock, this process may in fact select for rocks that have experienced lower water/rock ratios. Studying the deep gabbros at Oman, Bosch et al. (2004) reported elevated $^{87}Sr/^{86}Sr$ and low $\delta^{18}O$ in whole rocks (down to ~4‰), pargasite amphibole and clinopyroxene from coarse-grained leucocratic patches and dioritic dikes within 0–2 km of the Moho. Along with amphibole-plagioclase thermometry, the isotopic observations were interpreted as evidence for the influx of seawater from above at temperatures up to 1000 °C (Nicolas and Mainprice, 2005), which meets the preconditions for hydrous partial melting. Although it is not clear how seawater could physically migrate under these conditions, their results imply the formation of melts with mildly lower-$\delta^{18}O$ values than MORB at depths well below the dike-gabbro transition. Evaluation of $\delta^{18}O$(Zrn) in silicic rocks below the dike-gabbro transition at Oman would lend further insight into the representative role and extent of seawater during magmatism at deeper levels in the ocean crust.

5.5. $\delta^{18}O$ difference between MOR and ophiolite zircons

Relative to published $\delta^{18}O$(Zrn) for rocks in gabbroic portions of slow spreading oceanic crust, ophiolite plagiogranite extend to lower $\delta^{18}O$(Zrn) and the average value is shifted down by 0.3‰ (Fig. 7). Factors such as depth of magma intrusion, magma supply, tectonic setting (MOR versus subduction setting), and fluid sources (i.e., slab-derived fluids in subduction zones, meteoric fluids in Iceland, ocean water in mid-ocean ridge and suprasubduction spreading zones) could all contribute to subtle variations between published mid-ocean ridge plagiogranites and ophiolite plagiogranites. Differences in the petrogenetic process could also be important, but are not required. The majority of plagiogranite bodies from mid-ocean ridges are sampled from the gabbroic portions of slow spreading ocean crust, largely along fracture

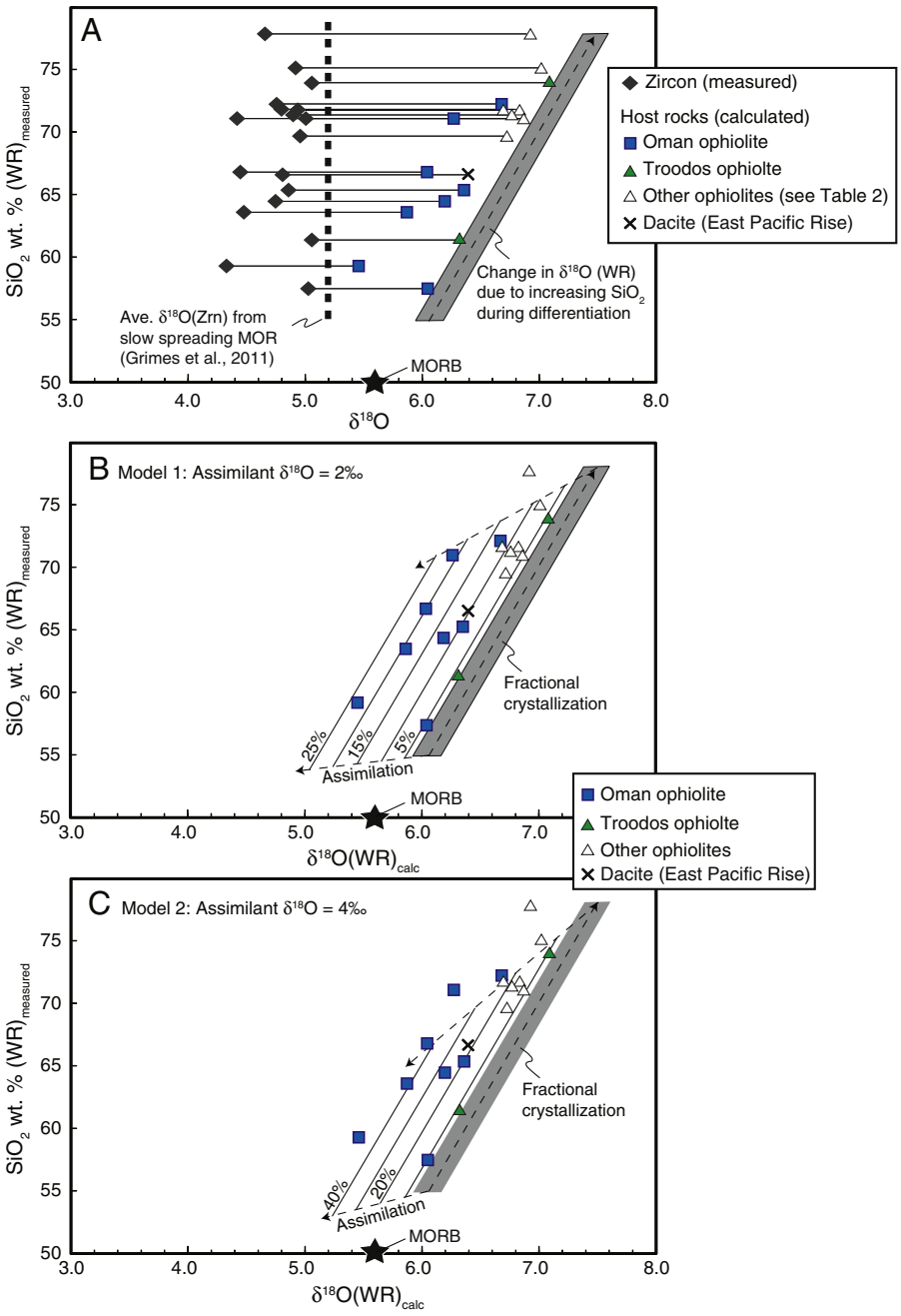

Fig. 13. A) Measured $\delta^{18}O$ values for zircon (rock-averaged values) and equilibrium $\delta^{18}O$ values calculated for parental magmas, plotted versus SiO_2 of the host rock. The $\delta^{18}O$ of parental magmas in equilibrium with zircon was calculated using the melt-zircon relation of Lackey et al. (2008) and measured SiO_2(WR) concentrations reported in Table 2. The gray bar depicts the $\delta^{18}O$ trend expected for fractional crystallization of plagioclase, olivine, pyroxene, and titanomagnetite from uncontaminated MORB (initial $\delta^{18}O(WR) = 5.6‰$) (i.e., Muehlenbachs and Byerly, 1982). B) Simple mixing model for bulk assimilation of hydrothermally altered mafic crust into a fractionating melt in $\delta^{18}O$ equilibrium with uncontaminated MORB. The gray bar is the same as in part A. Diagonal isopleths show the effect of variable percentages of contamination by an assimilant with $SiO_2 = 50$ wt.% and $\delta^{18}O(WR) = 2‰$; if the contaminant is a more siliceous partial melt derived from mafic rocks, the effect on SiO_2 would be less than is shown. The proportion of assimilant is shown in 5% increments, from 0 to 25%. C) Same as in B, except that the assimilant has $\delta^{18}O(WR) = 4‰$. The proportion of assimilant is shown in 10% increments, up to 40%.

zones and oceanic core complexes (e.g., Koepke et al., 2007). Oceanic core complexes represent the footwall to large offset (10s km) normal faults that denude gabbro and mantle peridotite and expose them directly on the seafloor. These settings lack the well-developed dike-gabbro transition that is suspected as a primary horizon for contamination in fast spreading ridges (e.g., McCaig and Harris, 2012), and drill core observations indicate the gabbroic crust is built by the intrusion of many narrow (<100 m thick) sill injections (Blackman et al., 2006; Grimes et al., 2008). Thermochronometry and spreading rate estimates for the Atlantis massif core complex, MAR suggest the multiply-intruded gabbroic crust was emplaced at depths of ~7 km (Grimes et al., 2011b; Schoolmeesters et al., 2012) before being denuded to the seafloor. Stable isotope studies indicate that the brittle portion of detachment faults serves as an effective conduit for fluid flow, but penetration into the footwall is concentrated within ~500 m of the fault (Alt and Bach, 2006; McCaig and Harris, 2012; McCaig et al., 2010) and migration of hydrothermal fluids carrying a seawater signature to the depth of magma intrusion is probably exceedingly limited. Even if small volume partial melts form at these depths, they would likely retain MORB-like $\delta^{18}O$. In contrast, the proximity of magma and an actively circulating hydrothermal system near the dike-gabbro transition, as in magmatically robust spreading centers envisioned during

formation of the Oman ophiolite and fast spreading ocean crust along the East Pacific Rise (e.g., France et al., 2009, 2010; Wanless et al., 2010, 2011), may produce relatively large volumes of partial melt with resolvable shifts to $\delta^{18}O$ lower than MORB-like values.

Aldiss (1981) initially noted that the volume of plagiogranite sampled by dredge and drilling of the seafloor is small compared to those observed in ophiolites, and we note that no large scale plagiogranite bodies like those found at Oman have been identified at a modern ridge. Dilek and Furnes (2011) discuss the sequence of crust formation within a suprasubduction zone ophiolite as being characterized by an initial stage of seafloor spreading and MORB-like magmatism, followed by the formation of hydrated arc-like magmas that intrude the existing crust. The development of oceanic lithosphere in this environment could serve as an ideal setting to promote partial melting and the generation of large plagiogranite intrusions. Along fast spreading ridges, where volcanism is robust, the dike-gabbro transition zone is typically covered by 1–2 km of extrusives and has rarely been drilled (e.g., Wilson et al., 2006); thus, it is possible that large plagiogranite intrusions also develop here but have yet to be sampled. Dacite lavas erupted from the East Pacific Rise carry a weak seawater signature (Wanless et al., 2011) and zircon from sample 265-70 (Table 1) yield similar $\delta^{18}O$ values (4.6–5.0‰) to ophiolite plagiogranite. Perhaps further exploration will lead to the discovery of large-scale silicic intrusions within this horizon at fast spreading mid-ocean ridges. If the difference in $\delta^{18}O$ is related to spreading rate (magma supply), it is consistent with other indicators of seawater-contamination such as elevated chlorine in basalt glasses from fast-spreading mid-ocean ridges (i.e. East Pacific Rise) and amphiboles in plutonic sections of ophiolites (i.e., Oman ophiolite) (Coogan, 2003; Coogan et al., 2003; Michael and Schilling, 1989).

5.6. Implications on the source of high $\delta^{18}O$ zircons in eclogite

The zircon-bearing rocks in oceanic crust characterized here serve as an analogue for the protolith of some zircon-bearing eclogites. In eclogite, zircon is often the only mineral to preserve magmatic-age information through the cycle of subduction and exhumation (e.g., Rubatto and Hermann, 2007) and is therefore used to constrain timing of different events (e.g., Bröcker and Keasling, 2006; Fu et al., 2013; Puga et al., 2005; Rubatto et al., 1999; Tomaschek et al., 2003). Distinguishing between igneous and metamorphic zircon is therefore a critical step for accurately interpreting the geologic history recorded in eclogites. Notably absent in all published ophiolite, mid-ocean ridge, and Iceland zircon populations are $\delta^{18}O$ values higher than the accepted mantle-like values (Fig. 7). High $\delta^{18}O$ values are observed in zircons from eclogite (e.g., Fu et al., 2009, 2013), however these are unlikely to reflect derivation from an igneous ocean crustal precursor. Considering the $\delta^{18}O$ constraints placed on igneous zircon from modern oceanic crust and ophiolites, igneous zircon in eclogites inherited directly from subducted oceanic crust should have $\delta^{18}O$ values at or mildly lower than the mantle-like range (Page et al., 2007b; Valley et al., 1998). Higher-$\delta^{18}O$ values are thus an effective indicator of new zircon growth during high-pressure metamorphism (i.e., metamorphic zircon), later remelting of high $\delta^{18}O$ source rocks within the subduction setting, or inheritance from continental source material as seen in the Oytag ophiolite.

Supplementary data to this article can be found online at http://dx.doi.org/10.1016/j.lithos.2013.07.026.

Acknowledgments

The authors thank the Division of Petrology and Volcanology, Department of Mineral Sciences, Smithsonian Institution for access to samples from the Oman ophiolite, from the collection of Debra Stakes. We thank Stakes for providing an additional Oman sample and helpful discussions during preparation of this manuscript, and Yao-Hui Jiang, Yu-Xiu Zhang, Michaela Kurth, Nik Christensen, Joshua Schwartz, Dorsey Wanless, and Serhat Köksal for access to zircons from additional ophiolites analyzed for this study. Brian Hess and Jim Kern assisted in sample preparation and polishing. Mike Spicuzza analyzed quartz aliquots from two Oman ophiolite samples. This research was partly supported by NSF (EAR0838058) and DOE (93ER14389). WiscSIMS is partially supported by NSF-EAR (0744079, 1053466).

Reviews by James Brophy, an anonymous reviewer, and editor-in-chief Nelson Eby aided in the preparation of this manuscript and were greatly appreciated.

Appendix A. Descriptions and field relations of ophiolite plagiogranite bodies sampled for this study

A.1. Northern Oman ophiolite (locations in Fig. 1A; abbreviated from Stakes and Taylor, 1992, 2003)

A.1.1. Suhaylay (OM81-80, OM81-83)

The plagiogranite near Suhaylay is the largest of those sampled, covering 10 km by 8 km in map area. This intrusion was emplaced stratigraphically deeper than other large bodies described below, with a lower contact within the lower cumulate gabbros. The upper contact varies from the dike-gabbro boundary to direct contact with basalts. The body is crosscut by a series of 1–3-m-thick mafic dikes that show variable degrees of recrystallization and exchange with the plagiogranite host. The lower contact of the plagiogranite is cut by hydrous, hornblende pegmatite dikes. Xenoliths of layered gabbros are present in the lower portion and even the core of the intrusion is again xenolith or enclave rich, which in places comprise up to 50% of the outcrop. Some xenoliths within the intrusion are partially recrystallized gabbro country rock, whereas others are described as 'net-veined ovoid pillows formed by quenching of the mafic melt within the plagiogranite liquid'. Mafic enclaves preserve a hornfelsic texture of equigranular brown actinolitic hornblende and sodic feldspar with little low-T hydrothermal overprint.

A.1.2. Aarja-Bayda (OM85-411, OM85-412)

Samples originate from a 1 to 2 km plagiogranite body that is crosscut by multiple generations of mafic dikes. Gabbroic wall rocks along the western margin have been metamorphosed to grades of hornblende to pyroxene hornfels. An extensive hydrothermal alteration aureole surrounds this body and extends hundreds of meters from the margin (Stakes and Taylor, 2003). The marginal gabbro is notably depleted in ^{18}O, reflecting alteration by high-temperature fluids. Primary plagioclase in the gabbro varies in composition from An_{71-89}. Secondary assemblages of sodic plagioclase (An_{20-26}) and actinolitic hornblende are compatible with temperatures in excess of 400 °C. Sample OM85-411 was collected near the lower contact with high-level gabbro, whereas sample OM85-412 was collected near the upper contact with sheeted diabase dikes. Xenoliths of basalt and granoblastic diabase are abundant within the plagiogranite intrusion, some of which have undergone partial digestion and extensive exchange with the plagiogranite magma. Several generations of dikes that are 0.5–1 m in width cut more than a third of the intrusion exposed in outcrop. Based on the field relations, Stakes and Taylor (2003) interpreted the basaltic dikes and plagiogranite magmas as being contemporaneous.

Although some xenoliths appear to originate from cross-cutting basaltic dikes, true xenoliths of preexisting gabbro and diabase are also present. These show partial digestion and extensive exchange with the plagiogranite magma. Stakes and Taylor (2003) interpret the field relations to indicate systematic recrystallization and assimilation of country rocks and late mafic dikes intruding the upper oceanic crust at the same time as the plagiogranite. They note no evidence of silicic feeder dikes for the intrusion.

A.1.3. Wadi Shafan (OM81-153, OM81-155, OM81-156, OM81-165)

Sampled from a transect described as "complex ocean crust" by Stakes and Taylor (1992). The plagiogranite body described from the Shafan area is a 2–3 km wide composite gabbro-plagiogranite intrusion that intrudes high-level gabbros and the lower part of the sheeted dike complex. It is intruded into a major shear zone, and was interpreted to represent a late stage feature intruded off-axis of the main spreading environment (Stakes and Taylor, 1992). Xenoliths of stoped diabase dikes are partially resorbed, and their margins are replaced by intergrowths of quartz and epidote. Gabbro around the margins of the intrusion is also highly altered. Stakes and Taylor (1992) describe low $\delta^{18}O$ values in the gabbros, diabase dikes, and quartz veins in the vicinity of this shear zone, focused near the contact with plagiogranite. A sample of gabbro and crosscutting dike sampled near the contact with plagiogranite record low $\delta^{18}O$ values of 4.8‰ and 2.9‰, respectively.

A.1.4. Wadi Rajmi (alternate spelling 'Ragmi') (OM81-75)

The Wadi Rajmi area represents a zone where intense fracturing and shearing accompanied crust formation, possibly representing a fossil transform fault (Stakes and Taylor, 1992). The zircon-bearing sample originates from a ~1 km wide plagiogranite body intruding the base of the sheeted dike complex. Several other plagiogranites in this area intrude the upper portion of the gabbro section. High-level gabbro near the lower contact with plagiogranite preserve mantle-like $\delta^{18}O(WR) = 5.8‰$.

A.1.5. Musafiyah body, near Haylayn (OM81-25)

The sample collected near Musafiyah contrasts with the others in that it was taken from a small segregation dike near the high-level gabbro-sheeted dike complex contact (Stakes and Taylor, 2003 their Fig. 6j). Stakes and Taylor (2003) note that over distances of a few tens of meters, these segregations can be traced upward to larger veins which coalesce into a single plagiogranite dike. The sample resembles the small, cm-scale segregation dikes that are frequently encountered in drilled sections of gabbroic crust from mid-ocean ridges (Niu et al., 2002; Blackman et al., 2006; Grimes et al., 2011a.

A.1.6. Lasail (OM85-519a)

There is a large late-stage intrusive with plagiogranite (~8 km diameter in map view) near the Lasail mining district; however this sample was collected approximately 15 km to the west within the high-level gabbros. It is a segregation plagiogranite dike similar to the one described from Musafiyah, and it intrudes pegmatitic gabbros up into the base of the sheeted dike complex.

A.2. Troodos, Cyprus

A.2.1. CG10–CY11

This sample was collected from a 1–2 m wide, irregular plagiogranite dike intruding sheeted diabase dikes and comprises primarily plagioclase + quartz. The sample was collected along highway E110 approximately 1.5 km N of Zoopigi. Latitude and Longitude: 34.86473 N, 33.01119 E.

A.2.2. CG10-CY3

This sample was collected from weathered pegmatitic gabbro pods (~30 cm diameter) within the gabbros below the Kakopetria detachment fault; the fault separates underlying gabbros from sheeted dikes above. The sample was collected approximately 15 m below the fault. The rock is dominantly plagioclase and large amphibole crystals (up to 2 cm long).

A.3. Fidalgo Island ophiolite, WA, USA

Samples ML-8 and ML-3 were collected from the Jurassic age Fidalgo Island ophiolite, WA (provided by Nik Christenson). The ophiolite comprises serpentinite at its base, with overlying layered gabbro, a mafic dike complex intruded by felsic (plagiogranite) dikes, mafic–felsic volcanic rocks, capped by pelagic sediments (Brown et al., 1979). One sample was taken from a decimeter-scale intrusion within amphibole-bearing gabbros. A second sample occurs as a 1 cm-wide dike intruding amphibole-bearing gabbro. Both host-rocks are dominated by quartz, plagioclase with trace amphibole, Fe–Ti oxides, and zircon.

A.4. Bay of Islands Ophiolite, Western Lewis Hills, Newfoundland (after Kurth et al., 1998)

Sample WLH-22 is described as trondhjemite intruding undeformed, mainly hornblende gabbros within the Coastal Complex of the Bay of Islands Ophiolite (Kurth et al., 1998). Zircons dated by multi-grain TIMS analysis yield an age of 503.7 ± 3.2 Ma, and whole rock initial εNd values were determined to be −1.5 to +2.0. The Western Lewis Hills have been interpreted as an island arc that was tectonically juxtaposed next to the Bay of Islands complex (e.g., Kurth et al., 1998).

A.5. Ekecikdag, Central Anatolia (after Köksal et al., 2010)

Samples EK-40 and EK-41 originate within dismembered ophiolite fragments in the Ekecikdag area of Central Anatolia, which formed in the Alpine Neotethys. These plagiogranite samples are tonalitic in composition, and contain quartz, plagioclase, hornblende, and biotite ± clinopyroxene. Based on field evidence and whole rock trace element characteristics, Köksal et al. (2010) interpreted them as forming in a suprasubduction zone setting.

A.6. Lagkor Lake ophiolite, Gerze, Tibet, China (after Zhang et al., 2007)

Plagiogranite sample GZ-45-1 was described by Zhang et al. (2007), and gave a SHRIMP Pb/U age of 166 ± 2.5 Ma. Plagiogranites in the Lagkor Lake ophiolite occur as cm- to meter-wide bodies hosted within amphibole-bearing gabbro; host-gabbros have undergone shearing and metamorphism at amphibolite facies. The plagiogranites are composed primarily of plagioclase, quartz, hornblende, and biotite. On the basis of field relations, and geochemical comparisons to other ophiolite plagiogranites these samples were interpreted to originate from hydrous partial melting of the gabbros during ductile shearing, within a spreading environment during the Jurassic.

A.7. Oytag ophiolite, northwest China (after Jiang et al., 2008)

The Oytag ophiolite is comprised of Carboniferous mafic volcanic rocks interbedded with chert, sheeted diabase dikes, plagiogranite (tonalite and trondhjemite), and rare ultrabasic rocks. The volcanics exhibit both transitional MORB and island arc geochemical characteristics (Jiang et al., 2008), and formation in an island arc setting is inferred on this basis. Plagiogranite intrudes the base of the volcanic rocks, and both are intruded by sheeted diabase dikes. The plagiogranites are composed of the primary minerals plagioclase, quartz, and amphibole, with secondary alteration to sericite, chlorite, and epidote. Flat to slightly depleted REE patterns of the Oytag plagiogranite relative to batch melting models of the nearby sheeted dikes were originally interpreted to indicate an origin by extensive fractional crystallization (58–85%) of a tholeiitic magma (Jiang et al., 2008).

A.8. Canyon Mountain ophiolite, OR, USA

The Canyon Mountain complex is part of the Blue Mountains Province of northeastern Oregon, and it has been interpreted as a volcanic-arc type ophiolite on the basis of geochemical, structural, and tectonic considerations (Gerlach et al., 1981; Misseri and Boudier, 1985).

Plagiogranite comprises the uppermost preserved portions of the ophiolite.

References

Alabaster, T., Pearce, J.A., Malpas, J., 1982. The volcanic stratigraphy and petrogenesis of the Oman ophiolite complex. Contributions to Mineralogy and Petrology 81, 168–183.

Aldiss, D.T., 1981. Oceanic plagiogranites from the ocean crust and ophiolites. Nature 289, 577–578.

Alt, J.C., Bach, W., 2006. Oxygen isotope composition of a section of lower oceanic crust, ODP Hole 735B. Geochemistry, Geophysics, Geosystems 7, G12008.

Alt, J.C., Teagle, D.A.H., Bach, W., Halliday, A.N., Erzinger, J., 1996. Stable and strontium isotopic profiles through hydrothermally altered upper oceanic crust, Hole 504B. In: Alt, J.C., Kinoshita, H., Stokking, L.B., Michael, P.J. (Eds.), Proc. ODP, Sci. Results, 148. Ocean Drilling Program, College Station, TX, pp. 57–69.

Amri, I., Benoit, M., Ceuleneer, G., 1996. Tectonic setting for the genesis of oceanic plagiogranites: evidence from a paleo-spreading structure in the Oman ophiolite. Earth and Planetary Science Letters 139, 177–194.

Anonymous, 1972. Penrose field conference on ophiolites. Geotimes 17, 24–25.

Barker, F., 1979. Trondhjemite: definition, environment, and hypotheses of origin. In: Barker, F. (Ed.), Trondhjemites, Dacites, and Related Rocks. Elsevier, Amsterdam, pp. 1–12.

Beard, J.S., Lofgren, G.E., 1991. Dehydration melting and water-saturated melting of basaltic and andesitic greenstones and amphibolites at 1, 3, and 6.9 kb. Journal of Petrology 32, 365–401.

Berndt, J., Koepke, J., Holtz, F., 2005. An experimental investigation of the influence of water and oxygen fugacity on differentiation of MORB at 200 MPa. Journal of Petrology 46, 135–167.

Bindeman, I.N., 2008. Oxygen isotopes in mantle and crustal magmas as revealed by single crystal analysis. Reviews in Mineralogy and Geochemistry 69, 445–478.

Bindeman, I.N., Gurenko, A., Carley, T., Miller, C., Martin, E., Sigmarsson, O., 2012. Silicic magma petrogenesis in Iceland by remelting of hydrothermally altered crust based on oxygen isotope diversity and disequilibria between zircon and magma with implications for MORB. Terra Nova 24, 227–232.

Blackman, D.K., Ildefonse, B., John, B.E., Ohara, Y., Miller, D.J., MacLeod, C.J., The Expedition 304/304 Scientists, 2006. Proceedings of the Integrated Ocean Drilling Program, 304/305. Integrated Ocean Drilling Program Management International, Inc., College Station, TX. http://dx.doi.org/10.2204/iodp.proc.304305.2006.

Bosch, D., Jamais, M., Boudier, F., Nicolas, A., Dautria, J.M., Agrinier, P., 2004. Deep and high temperature hydrothermal circulation in the Oman ophiolite—petrological and isotopic evidence. Journal of Petrology 45, 1181–1208.

Bouvier, A.-S., Ushikubo, T., Kita, N., Cavosie, A., Kozdon, R., Valley, J., 2012. Li isotopes and trace elements as a petrogenetic tracer in zircon: insights from Archean TTGs and sanukitoids. Contributions to Mineralogy and Petrology 163 (5), 745–768.

Bowman, J.R., Moser, D.E., Valley, J.W., Wooden, J.L., Kita, N.T., Mazdab, F., 2011. Zircon U–Pb isotope, $\delta^{18}O$ and trace element response to 80 m.y. of high temperature formation. American Journal of Science 311, 719–772.

Bröcker, M., Keasling, A., 2006. Ion probe U–Pb zircon ages from the high-pressure/low-temperature mélange of Syros, Greece: age diversity and the importance of pre-Eocene subduction. Journal of Metamorphic Geology 24, 615–631.

Brophy, J.G., 2009. La–SiO2 and Yb–SiO2 systematics in mid-ocean ridge magmas: implications for the origin of oceanic plagiogranite. Contributions to Mineralogy and Petrology 158, 99–111.

Brophy, J.G., Pu, X., 2012. Rare earth element–SiO_2 systematics of mid-ocean ridge plagiogranites and host gabbros from the Fournier oceanic fragment, New Brunswick, Canada: a field evaluation of some model predictions. Contributions to Mineralogy and Petrology 164, 191–204.

Brown, E.H., Bradshaw, J.Y., Mustoe, G.E., 1979. Plagiogranite and keratophyre in ophiolite on Fidalgo Island, Washington. Geological Society of America Bulletin 90, 493–507.

Cavosie, A.J., Kita, N.T., Valley, J.W., 2009. Mantle oxygen-isotope ratio recorded in magmatic zircon from the Mid-Atlantic Ridge. American Mineralogist 9, 926–934.

Coleman, R.G., Donato, M.M., 1979. Oceanic plagiogranite revisited. In: Barker, F. (Ed.), Trondhjemites, Dacites, and Related Rocks. Elsevier, Amsterdam, pp. 149–167.

Coleman, R.G., Peterman, Z.E., 1975. Oceanic plagiogranite. Journal of Geophysical Research 80, 1099–1108.

Coogan, L.A., 2003. Contaminating the lower crust in the Oman ophiolite. Geology 31, 1065–1068.

Coogan, L.A., Mitchell, N.C., O'Hara, M.J., 2003. Roof assimilation at fast spreading ridges: an investigation combining geophysical, geochemical, and field evidence. Journal of Geophysical Research 108 (B1). http://dx.doi.org/10.1029/2001JB001171.

Corfu, F., Hanchar, J.M., Hoskin, P.W.O., Kinny, P., 2003. Atlas of zircon textures. In: Hanchar, J.M., Hoskin, P.W.O. (Eds.), Reviews in Mineralogy and Geochemistry 53, 469–500.

Dilek, Y., Furnes, H., 2011. Ophiolite genesis and global tectonics: geochemical and tectonic fingerprinting of ancient oceanic lithosphere. Geological Society of America Bulletin 123, 387–411.

Dixon-Spulber, S., Rutherford, M.J., 1983. The origin of rhyolite and plagiogranite in oceanic crust: an experimental study. Journal of Petrology 24, 1–25.

Eiler, J.M., 2001. Oxygen isotope variations of basaltic lavas and upper mantle rocks. In: Valley, J.W., Cole, D.R. (Eds.), Reviews in Mineralogy and Geochemistry 43, 319–364.

Ernewein, M., Pflumio, C., Whitechurch, H., 1988. The death of an accretion zone as evidenced by the magmatic history of the Sumail ophiolite (Oman). Tectonophysics 151, 247–274.

Flagler, P.A., Spray, J.G., 1991. Generation of plagiogranite by amphibolite anatexis in oceanic shear zones. Geology 19, 70–73.

France, L., Ildefonse, B., Koepke, J., 2009. Interactions between magma and hydrothermal system in Oman ophiolite and in IODP Hole 1256D: fossilization of a dynamic melt lens at fast spreading ridges. Geochemistry, Geophysics, Geosystems 10, Q10O19.

France, L., Koepke, J., Ildefonse, B., Cichy, S., Deschamps, F., 2010. Hydrous partial melting in the sheeted dike complex at fast spreading ridges: experimental and natural observations. Contributions to Mineralogy and Petrology 160, 683–704.

France, L., Ildefonse, B., Koepke, J., 2013. Hydrous magmatism triggered by assimilation of hydrothermally altered rocks in fossil oceanic crust (northern Oman ophiolite). Geochemistry, Geophysics, Geosystems. http://dx.doi.org/10.1002/ggge.20137.

Fu, B., Valley, J.W., Kita, N.T., Spicuzza, M.J., Paton, C., Tsujimori, T., Bröker, M., Harlow, G.E., 2009. Origin of zircons in jadeitite. Contributions to Mineralogy and Petrology 159, 769–780.

Fu, B., Kita, N.T., Wilde, S.A., Liu, X., Cliff, J., Greig, A., 2013. Origin of the Tongbai–Dabie–Sulu Neoproterozoic low-$\delta^{18}O$ igneous province, east-central China. Contributions to Mineralogy and Petrology 165, 641–662.

Gautason, B., Muehlenbachs, K., 1998. Oxygen isotopic fluxes associated with high-temperature processes in the rift zones of Iceland. Chemical Geology 145, 275–286.

Gerlach, D.C., Ave Lallemant, H.G., Leeman, W.P., 1981. An island arc origin for the Canyon Mountain ophiolite complex, eastern Oregon, U.S.A. Earth and Planetary Science Letters 53, 255–265.

Gillis, K.M., 2008. The roof of an axial magma chamber: a hornfelsic heat exchanger. Geology 36, 299–302.

Gillis, K.M., Coogan, L.A., 2002. Anatectic migmatites from the roof of an ocean ridge magma chamber. Journal of Petrology 43, 2075–2095.

Godard, M., Bosch, D., Einaudi, F., 2006. A MORB source for low Ti magmatism in the Semail ophiolite. Chemical Geology 234, 58–78.

Gregory, R.T., Taylor Jr., H.P., 1981. An oxygen-isotope profile in a section of Cretaceous oceanic crust, Samail ophiolite, Oman: Evidence for $\delta^{18}O$ buffering of the oceans by deep (>5 km) seawater-hydrothermal circulation at mid-ocean ridges. Journal of Geophysical Research 86, 2737–2755.

Grimes, C.B., John, B.E., Cheadle, M.J., Wooden, J.L., 2008. Protracted construction of gabbroic crust at a slow-spreading ridge: Constraints from $^{206}Pb/^{238}U$ zircon ages from Atlantis Massif and IODP Hole U1309D (30°N MAR). Geochemistry, Geophysics, Geosystems 9, Q08012.

Grimes, C.B., John, B.E., Cheadle, M.J., Mazdab, F.K., Wooden, J.L., Swapp, S., Schwartz, J.J., 2009. On the occurrence, trace element geochemistry, and crystallization history of zircon from in situ ocean lithosphere. Contributions to Mineralogy and Petrology 158, 757–783.

Grimes, C.B., Ushikubo, T., John, B.E., Valley, J., 2011a. Uniformly mantle-like δ18O in zircons from oceanic plagiogranites and gabbros. Contributions to Mineralogy and Petrology 161, 13–33.

Grimes, C.B., Cheadle, M.J., John, B.E., Reiners, P.W., Wooden, J.L., 2011b. Cooling rates and depth of detachment faulting at oceanic core complexes: evidence from zircon Pb/U and (U–Th)/He ages. Geochemistry, Geophysics, Geosystems 12, Q0AG01.

Hattori, K., Muehlenbachs, K., 1982. Oxygen isotope ratios of the Icelandic crust. Journal of Geophysical Researches 87, 6559–6565.

Jiang, Y., Liao, S., Yang, W., Shen, W., 2008. An island arc origin of plagiogranites at Oytag, western Kunlun orogen, northwest China: SHRIMP zircon U–Pb chronology, elemental and Sr–Nd–Hf isotopic geochemistry and Paleozoic tectonic implications. Lithos 106, 323–335.

John, B.E., Foster, D.A., Murphy, J.M., Cheadle, M.J., Baines, A.G., Fanning, C.M., Copeland, P., 2004. Determining the cooling history of in situ lower ocean crust at Atlantis Bank, SW Indian Ridge. Earth and Planetary Science Letters 222, 145–160.

Kita, N.T., Ushikubo, T., Fu, B., Valley, J.W., 2009. High precision SIMS oxygen isotope analyses and the effect of sample topography. Chemical Geology 264, 43–57.

Koepke, J., Feig, S.T., Snow, J., Friese, M., 2004. Petrogenesis of oceanic plagiogranites by partial melting of gabbros: an experimental study. Contributions to Mineralogy and Petrology 146, 414–432.

Koepke, J., Berndt, J., Feig, S.T., Holtz, F., 2007. The formation of SiO_2-rich melts within deep oceanic crust by hydrous partial melting of gabbros. Contributions to Mineralogy and Petrology 153, 67–84.

Koepke, J., France, L., Müller, T., Faure, F., Goetze, N., Dziony, W., Ildefonse, B., 2011. Gabbros from IODP Site 1256, equatorial Pacific: insight into axial magma chamber processes at fast spreading ocean ridges. Geochemistry, Geophystems, Geosystems 12, Q09014.

Köksal, S., Goncuoglu, M.C., Toksoy-Koksal, F., 2010. Re-evaluation of the petrological features of the Ekecikdag oceanic plagiogranites in Central Anatolia/Turkey. METU convention, Oct. 8, 2010, Paper No. 46(9).

Kurth, M., Sassen, A., Suhr, G., Mezger, K., 1998. Precise ages and isotopic constraints for the Lewis Hills (Bay of Islands Ophiolite): preservation of an arc–spreading ridge intersection. Geology 26, 1127–1130.

Lackey, J.S., Valley, J.W., Chen, J.H., Stockli, D.F., 2008. Dynamic magma systems, crustal recycling, and alteration in the central Sierra Nevada Batholith: the oxygen isotope record. Journal of Petrology 49, 1397–1426.

Lippard, S.J., Shelton, A.W., Gass, I.G., 1986. The ophiolite of Northern Oman. Geological Society of London, Memoirs 11 (178 pp.).

MacLeod, C., Lissenberg, C., Bibby, L., 2013. "Moist MORB" axial magmatism in the Oman ophiolite: the evidence against a mid-ocean ridge origin. Geology 41, 459–462.

Manning, C.E., MacLeod, C.J., Weston, P.E., 2000. Lower-cracking front at fast-spreading ridges: evidence from the East Pacific Rise and the Oman ophiolite, in: ophiolites and oceanic crust: new insights from field studies and the Ocean Drilling Program. Special Paper—Geological Society of America 349, 261–272.

Mattey, D., Lowry, D., Macpherson, C., 1994. Oxygen-isotope composition of mantle peridotite. Earth and Planetary Science Letters 128, 231–241.

McCaig, A.M., Harris, M., 2012. Hydrothermal circulation and the dike-gabbro transition in the detachment mode of slow seafloor spreading. Geology 40, 367–370.
McCaig, A.M., Delacour, A., Fallick, A.E., Castelain, T., Früh-Green, G.L., 2010. Detachment fault control on hydrothermal circulation systems: interpreting the subsurface beneath the TAG hydrothermal field using the isotopic and geological evolution of oceanic core complexes in the Atlantic. American Geophysical Union Monograph 108, 207–240.
Michael, P.J., Schilling, J.-G., 1989. Chlorine in mid-ocean ridge magmas: evidence for assimilation of seawater-influenced components. Geochimica et Cosmochimica Acta 53, 3131–3143.
Misseri, M., Boudier, F., 1985. Structures in the Canyon Mountain Ophiolite indicate an island-arc intrusion. Tectonophysics 120, 191–209.
Muehlenbachs, K., 1986. Alteration of the ocean crust and the ^{18}O history of seawater. In: Valley, J.W., Taylor, H.P., O'Neil, J.R. (Eds.), Reviews in Mineralogy and Geochemistry 16, 425–444.
Muehlenbachs, K., Byerly, G., 1982. ^{18}O-enrichments of silicic magmas caused by crystal fractionation at the Galapagos spreading center. Contributions to Mineralogy and Petrology 79, 76–79.
Nicolas, A., Boudier, F., 2007. Comment on "dating the geologic history of Oman's Semail ophiolite: insights from U–Pb geochronology" by C. J. Warren, R. R. Parrish, D. J. Waters and M. P. Searle. Contributions to Mineralogy and Petrology 154, 111–113.
Nicolas, A., Mainprice, D., 2005. Burst of high-temperature seawater injection throughout accreting oceanic crust: a case study in Oman ophiolite. Terra Nova 17, 326–330.
Nicolas, A., Boudier, F., Ildefonse, B., Ball, E., 2000. Accretion of Oman and United Arab Emirates ophiolite: discussion of a new structural map. Marine Geophysical Researches 21, 147–179.
Nicolas, A., Boudier, F., Koepke, J., France, L., Ildefonse, B., Mevel, C., 2008. Root zone of the sheeted dike complex in the Oman ophiolite. Geochemistry, Geophysics, Geosystems 9, Q05001.
Niu, Y., Gilmore, T., Mackie, S., Greig, A., Bach, W., 2002. Mineral chemistry, whole-rock compositions, and petrogenesis of Leg 176 gabbros: data and discussion. In: Natland, J.H., Dick, H.J.B., Miller, D.J., Von Herzen, R.P. (Eds.), Proceedings of ODP, Scientific Results. , 176. Ocean Drilling Program, College Station, TX, pp. 1–60 ([Online] http://www-odp.tamu.edu/publications/176_SR/VOLUME/CHAPTERS/SR176_08.PDF).
Page, F.Z., Ushikubo, T., Kita, N.T., Riciputi, L.R., Valley, J.W., 2007a. High-precision oxygen isotope analysis of picogram samples reveals 2 μm gradients and slow diffusion in zircon. American Mineralogist 92, 1772–1775.
Page, F.Z., Fu, B., Kita, N.T., Fournelle, J., Spicuzza, M.J., Schulze, D.J., Viljoen, V., Basei, M.A.S., Valley, J.W., 2007b. Zircons from kimberlites: new insights from oxygen isotopes, trace elements, and Ti in zircon thermometry. Geochimica et Cosmochimica Acta 71, 3887–3903.
Pallister, J.S., Hopson, C.A., 1981. Samail ophiolite plutonic suite: field relations, phase variation, cryptic variation and layering, and a model of a spreading ridge magma chamber. Journal of Geophysical Research 86 (B4), 2593–2644.
Pallister, J.S., Knight, R.J., 1981. Rare earth element geochemistry of the Samail ophiolite near Ibra, Oman. Journal of Geophysical Research 86 (B4), 2673–2697.
Pearce, J.A., Robinson, P.T., 2010. The Troodos ophiolitic complex probably formed in a subduction initiation, slab edge setting. Gondwana Research 18, 60–81.
Pearce, J.A., Alabaster, T., Shelton, A.W., Searle, M.P., 1981. The Oman ophiolite as a Cretaceous arc–basin complex: evidence and implications. Philosophical Transactions of the Royal Society of London 300, 299–317.
Puga, E., Fanning, C.M., Nieto, J.M., Diaz De Federico, A., 2005. Recrystallization textures in zircon generated by ocean floor and eclogite-facies metamorphism: a cathodoluminescence and U–Pb SHRIMP study, with constraints from REE elements. The Canadian Mineralogist 43, 183–202.
Rollinson, H., 2008. Ophiolitic trondhjemites: a possible analogue for Hadean felsic 'crust'. Terra Nova 20, 364–369.
Rollinson, H., 2009. New models for the genesis of plagiogranites in the Oman Ophiolite. Lithos 112, 603–614.
Rubatto, D., Hermann, J., 2007. Zircon behavior in deeply subducted rocks. Elements 3, 31–35.
Rubatto, D., Gebauer, D., Compagnoni, R., 1999. Dating of eclogite-facies zircons: the age of Alpine metamorphism in the Sesia-Lanzo Zone (Western Alps). Earth and Planetary Science Letters 167, 141–158.
Schoolmeesters, N., Cheadle, M.H., John, B.E., Reiners, P.W., Gee, J., Grimes, C.B., 2012. The cooling history and the depth of detachment faulting at the Atlantis Massif oceanic core complex. Geochemistry, Geophysics, Geosystems 13, Q0AG12.
Schwartz, J.J., John, B.E., Cheadle, M.J., Wooden, J.L., Mazdab, F., Swapp, S., Grimes, C.B., 2010. Dissolution–reprecipitation of igneous zircon in mid-ocean ridge gabbro, Atlantis Bank, Southwest Indian Ridge. Chemical Geology 274, 68–81.
Spicuzza, M.J., Valley, J.W., Kohn, M.J., Girard, J.P., Fouillac, A.M., 1998. The rapid heating, defocused beam technique: a CO2-laser based method for highly precise and accurate determination of $\delta^{18}O$ values of quartz. Chemical Geology 144, 195–203.
Stakes, D.S., Taylor, H.P., 1992. The northern Samail ophiolite: an oxygen isotope, microprobe, and field study. Journal of Geophysical Research 97, 7043–7080.
Stakes, D.S., Taylor, H.P., 2003. Magmatic, metamorphic and tectonic processes in ophiolite genesis: oxygen isotope and chemical studies on the origin of large plagiogranite bodies in northern Oman, and their relationship to the overlying massive sulphide deposits. Geological Society of London Special Publication 218, 315–351.
Stakes, D., Mével, C., Cannat, M., Chaput, T., 1991. Metamorphic stratigraphy of Hole 735B. In: Von Herzen, R.P., Robinson, P.T. (Eds.), Proceedings of the Ocean Drilling Program Scientific Results. , 118, pp. 153–180.
Thy, P., Lesher, C.E., Mayfield, J.D., 1999. Low-pressure melting studies of basalt and basaltic andesite from the southeast Greenland continental margin and the origin of dacites at site 917. In: Larsen, H.C., Duncan, R.A., Allan, J.F., Brooks, K. (Eds.), Proceedings of the ODP, science research, vol. 163. Ocean Drilling Program, College Station, pp. 95–112.
Tilton, G.R., Hopson, C.A., Wright, J.E., 2012. Uranium–lead isotopic ages of the Samail Ophiolite, Oman, with applications to Tethyan ocean ridge tectonics. Journal of Geophysical Research 86, 2763–2775.
Tomaschek, F., Kennedy, A.K., Villa, I.M., Iagos, M., Ballhaus, C., 2003. Zircons from Syros, Cyclades, Greece—recrystallization and mobilization of zircon during high-pressure metamorphism. Journal of Petrology 44, 1977–2002.
Trail, D., Bindeman, I.N., Watson, E.B., Schmitt, A.K., 2009. Experimental calibration of oxygen isotope fractionation between quartz and zircon. Geochimica et Cosmochimica Acta 73, 7110–7126.
Tsuchiya, N., Shibata, T., Yoshikawa, M., Adachi, Y., Miyashita, S., Adachi, T., Nakano, N., Osanai, Y., 2013. Petrology of Lasail plutonic complex, northern Oman ophiolite, Oman: an example of arc-like magmatism associated with ophiolite detachment. Lithos 156, 120–138.
Valley, J.W., 2003. Oxygen isotopes in zircon. In: Hanchar, J.M., Hoskin, P.W.O. (Eds.), Reviews in Mineralogy and Geochemistry. , 53, pp. 343–385.
Valley, J.W., Kitchen, N., Kohn, M.J., Niendorf, C.R., Spicuzza, M.J., 1995. UWG-2, a garnet standard for oxygen isotope ratios: strategies for high precision and accuracy with laser heating. Geochimica et Cosmochimica Acta 59, 5223–5231.
Valley, J.W., Kinny, P.D., Schulze, D.J., Spicuzza, M.J., 1998. Zircon megacrysts from kimberlite: oxygen isotope heterogeneity among mantle melts. Contributions to Mineralogy and Petrology 133, 1–11.
Valley, J.W., Bindeman, I.N., Peck, W.H., 2003. Empirical calibration of oxygen isotope fractionation in zircon. Geochimica et Cosmochimica Acta 67, 3257–3266.
Valley, J.W., Lackey, J.S., Cavosie, A.J., Clechenko, C.C., Spicuzza, M.J., Basei, M.A.S., Bindeman, I.N., Ferreira, V.P., Sial, A.N., King, E.M., Peck, W.H., Sinha, A.K., Wei, C.S., 2005. 4.4 billion years of crustal maturation. Contributions to Mineralogy and Petrology 150, 561–580.
Wanless, V.D., Perfit, M.R., Ridley, W.I., Klein, E., 2010. Dacite petrogenesis on mid-ocean ridges: evidence for oceanic melting and assimilation. Journal of Petrology 51, 2377–2410.
Wanless, V.D., Perfit, M.R., Ridley, W.I., Wallace, P.J., Grimes, C.B., Klein, E.M., 2011. Volatile abundances and oxygen isotopes in basaltic to dacitic lavas on mid-ocean ridges: the role of assimilation at spreading centers. Chemical Geology 287, 54–65.
Warren, C.J., Parrish, R.R., Waters, D.J., Searle, M.P., 2005. Dating the geologic history of Oman's Semail Ophiolite: insights from U–Pb geochronology. Contributions to Mineralogy and Petrology 150, 403–422.
Warren, C.J., Searle, M.P., Parrish, R.R., Waters, D.J., 2007. Reply to Comment by F. Boudier and A. Nicolas on "Dating the geologic history of Oman's Semail Ophiolite: insights from U–Pb geochronology". Contributions to Mineralogy and Petrology 154, 115–118.
Wilson, D.S., et al., 2006. Drilling to gabbro in intact ocean crust. Science 312, 1016–1020.
Zhang, Y., Zhang, K., Li, B., Wang, Y., Wei, Q., Tang, X., 2007. Zircon SHRIMP U–Pb geochronology and petrogenesis of the plagiogranites from the Lagkor Lake ophiolite, Gerze, Tibet, China. Chinese Science Bulletin 52, 651–659.